INTERNATIONAL INSTITUTE FOR HYDRAULIC AND ENVIRONMENTAL ENGINEERING

DELFT NETHERLANDS

Prof. dr ir J.A. Battjes

SHORT WAVES

SHORT WAVES

1. Introduction

1.1. Aim and scope

The course "short waves" deals with a class of gravity surface waves in water. Such waves can broadly be classified into two categories, depending on the ratio of a typical wavelength (L) to the mean water-depth (h). If L/h is much greater than 1 (L/h >>), we speak of "long waves". If L/h is not much greater than 1, we speak of "short waves". Tides, and flood waves in rivers, are examples of long waves. Wind-generated waves and ship-waves are examples of short waves.

There are certain differences in the properties of long waves and short waves which have led to different mathematical theories, for which reason the two categories are usually treated separately. For a treatment of long waves, reference is made to the course on nearly-horizontal flows. As the name implies, the present course deals with short waves. Its aim is to give an introduction to the hydrodynamic aspects of such waves, with applications in coastal and harbour engineering.

The present course is restricted to long-crested, periodic waves. Wind-generated waves are more complicated in structure and appearance. Their description requires spectral and statistical methods, which are not treated here. Instead, reference is made to a special course on those topics.

The treatment adopted in this course holds a middle course between a one-sided emphasis on fundamentals, and an exclusive cook-book style of presenting recipes. The mathematical theory of sinusoidal, progressive waves is presented in some detail, since that is basic for an understanding of wave phenomena. More complicated situations are treated with less mathematics, either because it is not available (wave breaking) or it is deemed to be outside the scope of this course (wave diffraction). Calculus and elementary fluid mechanics are supposed to be known.

1.2. Long waves vs. short waves, and their relation to other classes of flows in hydraulics

Different classes of flows in hydraulics can be distinguished, depending mainly on the relative importance of the various terms in the momentum balance.

As regards the balance of vertical momentum, a major distinction can be made between flows in which the vertical accelerations are absent or negligible, and flows in which they are significant. In steady-flow open-channel hydraulics, these classes of flows are referred to as uniform or gradually varied steady flows (backwater curves), and rapidly varied steady flows (flow through an orifice, over a weir crest, etc.).

In gradually varied flows, the rate of change of velocity with distance is low, by definition. In other words, the radius of curvature of the streamlines in the vertical plane is large compared to the flow depth. This implies that the vertical accelerations are insignificant, and that the pressure distribution is virtually hydrostatic. Thus, the wave-induced pressure is uniform throughout the vertical. The pressure gradients which accelerate or decelerate the flow horizontally tend to create and maintain a vertically uniform profile of horizontal velocity. Although this implies the development of bed resistance, and a boundary layer type departure from uniformity of the velocity profile, it is nevertheless meaningful to deal with the vertically-average flow velocity. Thus, the vertical coordinate is effectively eliminated from the problem as an independent variable.

In rapidly varied flow, the situation with respect to all of the aspects referred to above is just the opposite.

The differences between gradually varied and rapidly varied steady flows are the same as those between long waves and short waves respectively. (Indeed, long waves are nothing but unsteady, gradually varied flows). They have been collected in Table 1.1 and illustrated in Fig. 1.1.

Flow property	Gradually varied steady flows, and long waves	Rapidly varied steady flows, and short waves
Vertical curvature of streamlines	Weak	Strong
Vertical acceleration	Insignificant	Significant
Pressure distribution	Approx. hydrostatic	Significantly non-hydrostatic
Flow velocity profile	Approx. uniform (apart from bottom-induced boundary layer)	Significantly non-uniform
Bed resistance	Significant	Insignificant

Table 1.1

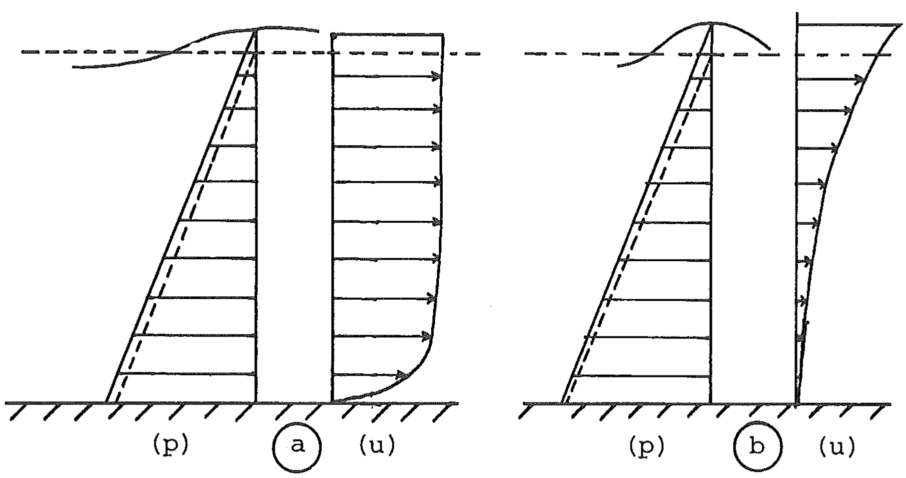

Fig. 1.1. Pressure (p) and velocity (u) profiles in long waves (a) and short (b)

1.3. Assumptions in theory for short waves

In the following chapters, only the most elementary theory of short waves will be presented. In other words, all effects which are not essential to the phenomenon of short gravity surface waves in water will be ignored. This leads to the following set of assumptions:

- non-viscous fluid of constant density (incompressible and homogeneous) in field of gravity
- stress-free upper surface
- no surface tension
- rigid, impermeable, horizontal bottom
- periodic, long-crested waves which progress without change in shape

1.4. Parameters

The independent parameters which are sufficient to describe the wave motion corresponding to the preceding assumptions (except for an arbitrary, uniform velocity of translation) are listed below:

- mass density (ρ)
- gravity acceleration (g)
- mean depth (h)
- wave height (H)
- wave length (L)

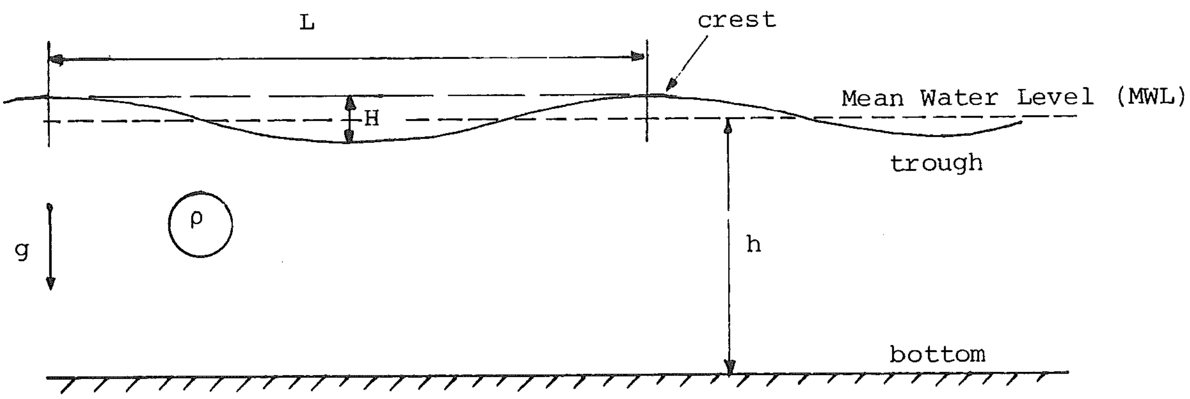

Fig. 1.2.

The relative depth h/L is important with respect to the effect of the bottom on the wave motion, as indicated in the preceding paragraphs. The ratio H/L, the so-called wave steepness, is a measure of the relative intensity of the wave motion. It cannot exceed a certain limiting value of the order of 10^{-1}, because of wave breaking.

In order to describe the wave motion in a unique manner, we must specify a reference system. We will choose it such that relative to that system, the horizontal velocity below the level of the wave troughs has an average value equal to zero. We use orthogonal axes, with the x-axis horizontal, positive in the direction of wave advance, and with the z-axis positive upwards, with z=0 in the mean water level (MWL), as indicated in Figure 1.3. The free surface elevation

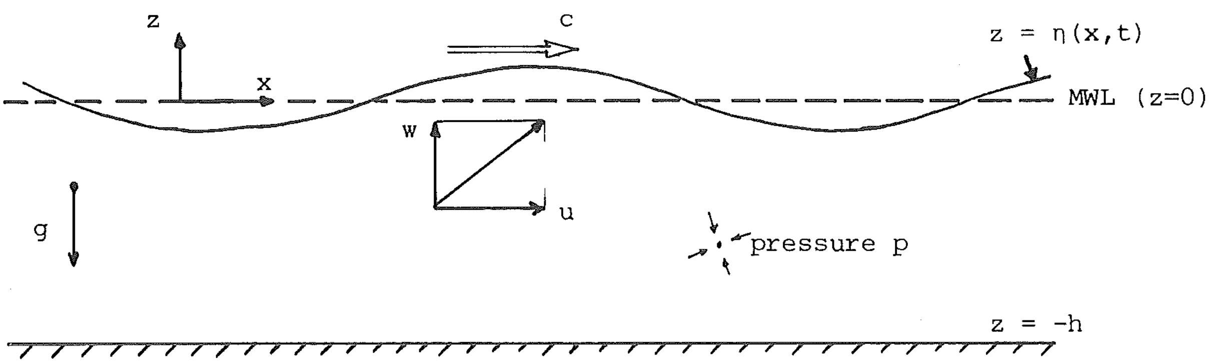

Fig. 1.3

above MWL is denoted by η, so that the equation of the free surface is $z=\eta(x,t)$, in which t is time. This equation can be reduced to a simpler form by recognizing that the wave form advances with a speed (say c) in the positive x-direction:

$$z=\eta\ (x - ct) \tag{1.1}$$

The time between passage of successive wave crests past a point x=const is called the wave period, written as T, which is related to L and c by the identity

$$L= c\,T \tag{1.2}$$

Note that L is independent of our choice of reference system, whereas c and T are not.

The dependent variables characterizing the flow field are the x- and z-components of the flow velocity, and the pressure, denoted as u, w and p respectively.

2. Basic equations

In this chapter, the basic equations governing the wave motion under the assumptions listed above will be formulated.

2.1. Condition of incompressibility

It follows from the assumed incompressibility of the water that the net volume flow through an arbitrary, submerged closed control surface must be zero. Equivalently, we can say that the volumetric strain rate must be zero. Both viewpoints lead to the following constraint on the velocity field (in two dimensions):

$$\frac{\partial u}{\partial x} + \frac{\partial w}{\partial z} = 0 \tag{2.1}$$

2.2. Dynamic equation

A statement of Newton's second law of motion should in the case considered here include only pressure gradients and gravity as force terms. This leads to

$$\frac{du}{dt} = -\frac{1}{\rho}\frac{\partial p}{\partial x} \tag{2.2x}$$

$$\frac{dw}{dt} = -\frac{1}{\rho}\frac{\partial p}{\partial z} - g \tag{2.2z}$$

The symbol $\frac{du}{dt}$ denotes a total acceleration, as experienced by a fluid particle. It consists of a local contribution, expressing the temporal change of velocity in a fixed point, and a convective contribution, expressing the variation in flow velocity at fixed time between neighbouring points in space. In other words, the convective term arises because the particle moves into a region where the velocity is different from where it was initially. This is written as follows, recognizing that x=x(t), z=z(t) if we follow a particle:

$$\frac{du}{dt} = \frac{\partial u}{\partial t} + \frac{\partial u}{\partial x}\frac{dx}{dt} + \frac{\partial u}{\partial z}\frac{dz}{dt}$$

Following a particle implies $\frac{dx}{dt} = u$ and $\frac{dz}{dt} = w$, so that

$$\underbrace{\frac{du}{dt}}_{\text{total}} = \underbrace{\frac{\partial u}{\partial t}}_{\text{local}} + \underbrace{u\frac{\partial u}{\partial x} + w\frac{\partial u}{\partial z}}_{\text{convective}} \tag{2.3x}$$

and similarly for $\frac{dw}{dt}$:

$$\frac{dw}{dt} = \frac{\partial w}{\partial t} + u\frac{\partial w}{\partial z} + w\frac{\partial w}{\partial z} \tag{2.3z}$$

The equations (2.2x) and (2.2z) do not have a symmetric form, because of the appearance of g in (2.2z). The two equations can be written in a similar form by substituting $g = \frac{\partial}{\partial z}(gz)$ in (2.2z), and by adding a zero-term $\frac{\partial}{\partial x}(gz)$ to (2.2x). Together with a substitution of (2.3), and using the fact that ρ = constant, this gives

$$\frac{\partial u}{\partial t} + u\frac{\partial u}{\partial x} + w\frac{\partial u}{\partial z} + \frac{\partial}{\partial x}\left(\frac{p}{\rho} + gz\right) = 0 \tag{2.4x}$$

and

$$\frac{\partial w}{\partial t} + u\frac{\partial w}{\partial x} + w\frac{\partial w}{\partial z} + \frac{\partial}{\partial z}\left(\frac{p}{\rho} + gz\right) = 0 \tag{2.4z}$$

2.3. Boundary conditions

We will state only boundary conditions at the free surface and at the bottom. (For a complete formulation, conditions at lateral boundaries should be specified also, which in the case considered here take the form of a statement of spatial periodicity.)

Kinematic boundary conditions for a non-viscous fluid merely state that no fluid particles cross a surface bounding the fluid. This gives

$$w=0 \quad \text{at } z=-h \tag{2.5}$$

and

$$\frac{d\eta}{dt} = w \quad \text{at } z=\eta(x,t)$$

which can be expanded in a manner similar to (2.3):

$$\frac{\partial \eta}{\partial t} + u\frac{\partial \eta}{\partial x} = w \quad \text{at } z=\eta(x,t) \tag{2.6}$$

Dynamic boundary conditions deal with stresses. The bottom is assumed to be rigid, for which reason no dynamic boundary condition needs to be given at the bottom. The condition of a stress-free upper surface can be written as

$$p=0 \quad \text{at } z=\eta(x,t) \tag{2.7}$$

(The fact that the shear stresses at the surface are zero need not be stated since the fluid is assumed to be non-viscous, which is to say that shear stresses are zero everywhere.)

2.4. Condition of irrotationality

Due to the velocity gradients, fluid particles can rotate about their axes as they move. The velocity of rotation in the (x,z)-plane is

$$\Omega_y = \tfrac{1}{2}\left(\frac{\partial w}{\partial x} - \frac{\partial u}{\partial z}\right) \qquad (2.8)$$

Under the conditions assumed (in particular: no viscosity), it can be shown that the rotation of each fluid particle is constant:

$$\frac{d\Omega_y}{dt} = 0 \qquad (2.9)$$

(Conservation of angular momentum.) Therefore, motions starting from rest, in which initially $\Omega_y = 0$ for all particles, will be irrotational:

$$\Omega_y = \tfrac{1}{2}\left(\frac{\partial w}{\partial x} - \frac{\partial u}{\partial z}\right) = 0 \qquad (2.10)$$

(Note: in a real (viscous) fluid, rotation can be generated at the boundaries. Due to the oscillatory nature of the flow under waves, the wave-induced boundary layer thickness remains relatively small. Outside that thin layer, the wave-induced motion is virtually irrotational. This is a more satisfactory justification for (2.10) than the reasoning given above, which was based on the assumption of zero viscosity.)

The condition of irrotationality ensures the existence of a scalar function, the so-called velocity potential, written as ϕ, such that its derivative in any one direction equals the component of flow velocity in that direction:

$$u = \frac{\partial \phi}{\partial x} \; , \; w = \frac{\partial \phi}{\partial z} \qquad (2.11)$$

This potential has no obvious physical meaning, but its use simplifies the mathematics because an unknown vector quantity (the velocity) is replaced by an unknown scalar quantity (the potential).

Substitution of (2.11) into (2.1) gives

$$\frac{\partial^2 \phi}{\partial x^2} + \frac{\partial^2 \phi}{\partial z^2} = 0 \qquad (2.12)$$

which is the so-called Laplace equation.

Substitution of (2.10) and (2.11) into (2.4x) gives

$$\frac{\partial}{\partial t}\left(\frac{\partial \emptyset}{\partial x}\right) + u\frac{\partial u}{\partial x} + w\frac{\partial w}{\partial x} + \frac{\partial}{\partial x}\left(\frac{p}{\rho} + \partial z\right) = 0$$

or

$$\frac{\partial}{\partial x}\{ox\left(\frac{\partial \emptyset}{\partial t}\right) + \tfrac{1}{2}\,ox\,(u^2 + w^2) + \left(\frac{p}{\rho} + gz\right)\} = 0 \qquad (2.13x)$$

A similar equation is obtained from (2.4z). This implies that the quantity in the brackets has the same value throughout the fluid. In an undisturbed region, it equals zero because each of the three terms in parentheses is zero there. Therefore, the quanity in the brackets is zero everywhere:

$$ox\,\frac{\delta\phi}{\delta t} + \tfrac{1}{2}\,ox(u^2 + w^2) + \left(\frac{p}{\rho} + g.z\right) = 0 \qquad (2.14)$$

This is the so-called Bernoulli equation for unsteady flow.

Finally (2.11) can be substituted into the boundary conditions, which gives

$$\frac{\partial \emptyset}{\partial z} = 0 \qquad \text{at } z = -h \qquad (2.15)$$

$$\frac{\partial \eta}{\partial t} + \frac{\partial \emptyset}{\partial x}\frac{\partial \eta}{\partial x} = \frac{\partial \emptyset}{\partial z} \qquad \text{at } z = \eta\,(x,t) \qquad (2.16)$$

and

$$\frac{\partial \emptyset}{\partial t} + \tfrac{1}{2}\left\{\left(\frac{\partial \emptyset}{\partial x}\right)^2 + \left(\frac{\partial \emptyset}{\partial z}\right)^2\right\} + g\eta = 0 \qquad \text{at } z = \eta\,(x,t) \qquad (2.17)$$

2.5. Linearization

Despite the simplification obtained by the introduction of a velocity potential, it has not yet been possible to obtain an exact solution to the preceding equations in closed form for a periodic wave. This is due to the nonlinear character of the free surface conditions (2.16) and (2.17). Not only do these equations contain product terms of dependent variables, but they have the added complexity of being prescribed at the free surface, which itself is an unknown.

However, many approximate solutions are available. The simplest one is based on the assumptions of relatively low waves ($H/L \ll 1$ and $H/h \ll 1$), in which case the nonlinear quadratic terms in the free surface conditions are small compared to the linear ones, and the difference in instantaneous elevation of the free surface ($z=\eta$) and its mean value ($z=0$) is negligible as far as the boundary conditions are concerned. Introducing these approximations in (2.16) and (2.17) gives

$$\frac{\partial \phi}{\partial z} = \frac{\partial \eta}{\partial t} \qquad \text{at } z=0 \tag{2.18}$$

and

$$\frac{\partial \phi}{\partial t} + g\eta = 0 \qquad \text{at } z=0 \tag{2.19}$$

A solution of the linearized equations, representing a progressive wave, will be investigated in chapter 3. A review of some nonlinear approximations is given in chapter 4.

3. Linear theory of waves in constant depth

3.1. Surface profile

The linearized set of equations presented in chapter 2 has constant coefficients, so that it admits sinusoidal waves as a solution. We will in this chapter analyse such solution, starting from an assumed sinusoidal profile progressing at a constant speed in the positive x-direction. Using the symbols defined in chapter 1, the equation of the free surface (1.1) can be written as

$$\eta(x,t) = -\frac{1}{2}H\sin\left\{2\pi\left(\frac{x-ct}{L}\right)\right\} \tag{3.1}$$

or, using (1.2),

$$\eta(x,t) = \frac{1}{2}H\sin\left(\frac{2\pi}{T}t - \frac{2\pi}{L}x\right) \tag{3.2}$$

For brevity of notation, we now introduce

. the elevation amplitude:

$$a = \frac{1}{2}H \tag{3.3}$$

. the wave number:

$$k = \frac{2\pi}{L} \tag{3.4}$$

. the (angular) wave frequency:

$$\omega = \frac{2\pi}{T} \tag{3.5}$$

. the phase:

$$S(x,t) = \frac{2\pi}{T}t - \frac{2\pi}{L}x = \omega t - kx \tag{3.6}$$

Using these, (3.2) can be written as

$$\eta(x,t) = a\sin(\omega t - kx) = a\sin S(x,t) \tag{3.7}$$

and (1.2) as

$$c = \frac{\omega}{k} \tag{3.8}$$

The wavenumber k represents the phase change per unit propagation distance (at a given instant), and the wave frequency represents the phase change per unit time (at a fixed point). An observer, travelling with velocity V, would see a phase increase per unit time given by

$$\frac{\partial S}{\partial t} + \frac{\partial S}{\partial x}\frac{dx}{dt} = \frac{\partial S}{\partial t} + V\frac{\partial S}{\partial x} = \omega - Vk \qquad (3.9)$$

If he would travel along with the wave form, e.g. by keeping up with a wave crest, he would observe no phase change at all. It follows from (3.9) that the velocity required for this to happen is ω/k, i.e. the velocity c. This is no surprise, of course, since c was defined as the velocity of the wave form. The preceding viewpoint was offered to emphasize that c represents the velocity of points of constant phase, for which reason it is called the phase velocity.

3.2. Velocity potential

In this and the following paragraphs, we will investigate the flow properties associated with the given surface profile (3.7). The kinematic equations will be considered first, without giving any consideration to the dynamics. The reason for making this separation explicit, apart from the wish to work systematically, is that the kinematic solution applies to waves in constant depth with a variety of dynamic surface conditions (e.g., internal waves, waves under an ice cover, waves being influenced by surface tension, etc.). Therefore, the results have a greater degree of generality than would have been the case if a specific dynamic boundary condition, such as (2.19), would have been used from the outset.

A resume of the kinematic equations is given below.

$$z=0 \longrightarrow \frac{\partial \phi}{\partial z} = \frac{\partial \eta}{\partial t} \qquad (2.18)$$

$$\frac{\partial^2 \phi}{\partial x^2} + \frac{\partial^2 \phi}{\partial z^2} = 0 \qquad (2.12)$$

$$z=-h \longrightarrow \frac{\partial \phi}{\partial z} = 0 \qquad (2.15)$$

We seek a solution for ϕ satisfying these equations, for a progressive wave represented by (3.7). The solution for ϕ must vary sinusoïdally with x and t, although not necessarily in phase with η, and we must allow for a variation of the amplitude of ϕ, written as $\hat{\phi}$, with z. Therefore, we try a solution of the form

$$\phi(x,z,t) = \hat{\phi}(z) \sin(\omega t - kx + \alpha) \qquad (3.10)$$

where $\hat{\phi}(z)$ and α are to be determined. To this end, we substitute (3.10) into (2.12), with the result

$$\left(\frac{d^2\hat{\phi}}{dz^2} - k^2\ \hat{\phi}\right) \sin\ (\omega t\ -\ kx\ +\ \alpha)\ =\ 0 \tag{3.11}$$

This equation must hold for arbitrary x and t, which implies that

$$\frac{d^2\hat{\phi}}{dz^2} - k^2\ \hat{\phi} = 0 \tag{3.12}$$

This is a linear, second-order ordinary differential equation with constant coefficients. Its general solution therefore is the sum of two exponential functions:

$$\hat{\phi}(z) = A_1\, e^{kz} + A_2\, e^{-kz} \tag{3.13}$$

in which A_1 and A_2 are constants, whose values are determined by the boundary conditions. Use of the bottom boundary condition (2.15) gives

$$\left.\frac{d\hat{\phi}}{dz}\right|_{z=-h} = A_1\ k\ e^{-kh} - A_2\ k\ e^{-kh} = 0 \tag{3.14}$$

or

$$A_2 = A_1\ e^{-2\ kh} \tag{3.15}$$

so that (3.13) can be written as

$$\hat{\phi}(z) = 2\ A_1\ e^{-kh}\ \cosh\ k(h+z) \tag{3.16}$$

Substitution of (3.7) and (3.16) into the kinematic surface condition (2.18) gives

$$2A_1 e^{-kh}\ k\ \sinh\ kh\ \sin\ (\omega t\ -\ kx\ +\alpha) = \omega a\ \cos\ (\omega t\ -\ kx) \tag{3.17}$$

from which it follows that

$$2A_1 k\ e^{-kh}\ \sinh\ kh = \omega a \tag{3.18}$$

and

$$\alpha = \frac{\pi}{2} \tag{3.19}$$

Finally, substitution of the results (3.16), (3.18) and (3.19) into (3.10) yields the following expression for the velocity potential:

$$\boxed{\phi(x,z,t) = \frac{\omega a}{k}\,\frac{\cosh\ k(h+z)}{\sinh\ kh}\ \cos\ (\omega t\ -\ kx)} \tag{3.20}$$

3.3. Particle velocities

Partial differentiation of ϕ with respect to x and z, respectively, gives

$$\frac{\partial\phi}{\partial x} = u = \omega a \frac{\cosh k(h+z)}{\sinh kh} \sin(\omega t - kx) \tag{3.21}$$

and

$$\frac{\partial\phi}{\partial z} = w = \omega a \frac{\sinh k(h+z)}{\sinh kh} \cos(\omega t - kx) \tag{3.22}$$

or

$$u = \hat{u} \sin S \quad \text{and} \quad w = \hat{w} \cos S \tag{3.23}$$

in which the amplitudes $\hat{u}$ and $\hat{w}$ are given by

$$\hat{u} = \omega a \frac{\cosh k(h+z)}{\sinh kh} \tag{3.24}$$

and

$$\hat{w} = \omega a \frac{\sinh k(h+z)}{\sinh kh} \tag{3.25}$$

It appears from the above that u and w in any fixed point are 90° out of phase. This implies a rotation of the velocity vector.

In order to investigate the variation of the velocity amplitudes with z, we first consider their values near the surface (z=0) and near the bottom (z=-h):

$$\hat{u} = \omega a/\tanh kh \quad \text{and} \quad \hat{w}=\omega a \quad \text{at} \quad z=0 \tag{3.26}$$

$$\hat{u} = \omega a/\sinh kh \quad \text{and} \quad \hat{w}=0 \quad \text{at} \quad z=-h \tag{3.27}$$

The relative magnitudes of $\hat{u}$ near the surface and near the bottom are dependent on kh only, in other words on the ratio h/L.

If kh>>1 (so-called deep water) and if also k(h+z)>>1 (the upper region of the deep water), we can approximate the hyperbolic functions in (3.24) and (3.25) with exponential functions. This is because $\cosh x = \frac{1}{2}(e^x + e^{-x}) = \frac{1}{2} e^x (1 + e^{-2x})$. If x>>1, e^{-2x} <<1, in which case $\cosh x \simeq \frac{1}{2} e^x$. The same holds for sinh x. (This approximation is already good to well within 1% if $x > 3$.) Therefore, in the upper region of deep water, (3.24) and (3.25) can be approximated as

$$\hat{u} \simeq \hat{w} \simeq \omega a\, e^{kz} \quad \text{(in deep water)} \tag{3.28}$$

The condition "deep water" or "kh>>1" is often taken to be $kh \gtrsim 3$, or $h/L \gtrsim \frac{1}{2}$.

If $kh \ll 1$ (so-called shallow water), which implies $k(h+z) \ll 1$ for all points below MWL, the hyperbolic functions in (3.24) and (3.25) can be approximated differently, using the fact that $\cosh x \simeq 1$ and $\sinh \simeq x$ for $x \ll 1$. We then obtain the following approximations to (3.24) and (3.25):

$$\hat{u} = \frac{\omega a}{kh} = c\,\frac{a}{h} \quad \text{and} \quad \hat{v} = \omega a\,(1+\frac{z}{h}) \quad \text{for } kh \ll 1 \qquad (3.29)$$

The condition "shallow water" or "$kh \ll 1$" is often taken to be $kh \lesssim \frac{1}{3}$, or $h/L \lesssim \frac{1}{20}$.

In the shallow-water approximation, the horizontal velocity does not vary with z. In other words, a long-wave property is here recovered as a special case (shallow water) of the short-wave theory.

Notice that in shallow water ($kh \ll 1$), $\hat{u} = (\omega a)/(kh) \gg \omega a$. Thus, a wave of given elevation amplitude and frequency causes larger horizontal velocities if it is in shallower water. This is of importance with regard to sediment transport, or wave-induced loads on structures.

A schematic drawing of vertical profiles of $\hat{u}$ is given in figure 3.1.

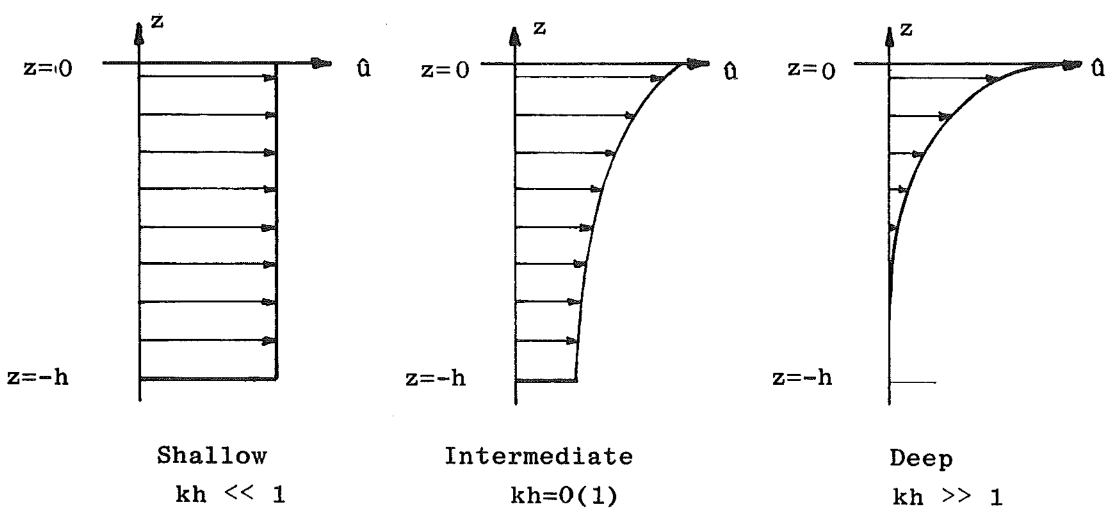

Figure 3.1

3.4. Particle paths

The equations given above enable us to calculate how the velocity in a fixed point (constant x,z) varies with time. In this paragraph we consider a given particle. In a physical experiment, we would do that by labeling a particle, e.g. by introducing a small, neutrally buoyant opaque, solid particle into the water. In a mathematical description, we must also label the particle which we want to follow, e.g. by its coordinates (x_o, z_o) at some previous time, or, for oscillatory motion, the coordinates of the mean position.

The displacements in the x- and z-direction from the mean particle position (x_o, z_o) are denoted as $\chi(t)$ and $\zeta(t)$. Reference is made to figure 3.2.

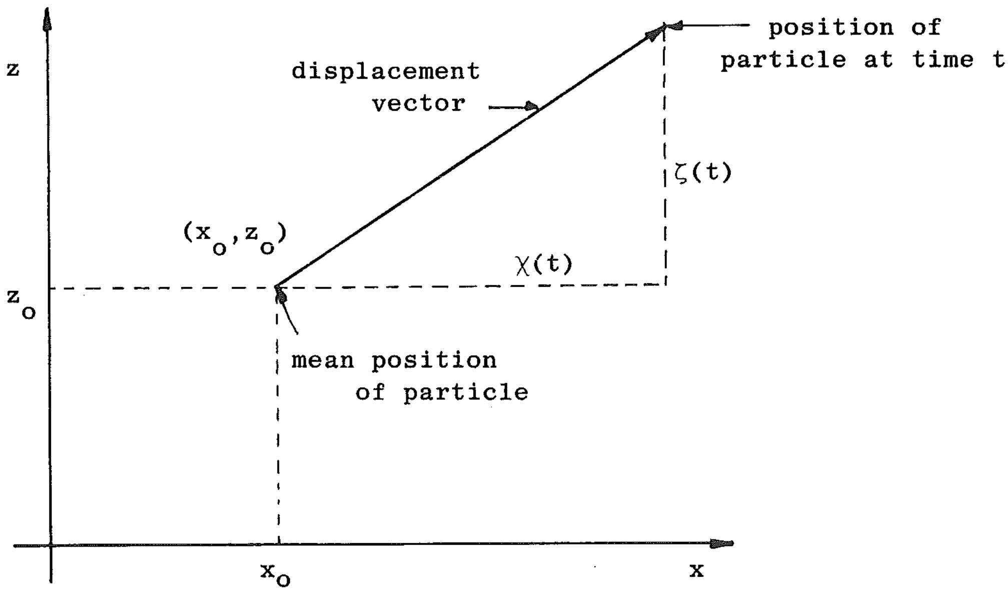

Figure 3.2

The displacements are equal to the time integral of the particle velocity components. For relatively small displacements, as has already been assumed, the actual particle velocity is approximately equal to the velocity at its mean position at the same time. Thus,

$$\chi(t') \simeq \int^{t'} u(x=x_o, z=z_o, t)\,dt \tag{3.30}$$

and likewise for $\zeta(t)$. Substitution of the preceding equations for u and w gives

$$\chi(t) = -\hat{\chi} \cos (\omega t - kx_o) \tag{3.31}$$

and

and

$$\zeta(t) = \hat{\zeta} \sin (\omega t - kx_o) \tag{3.32}$$

in which

$$\hat{\chi} = \frac{\hat{u}}{\omega} = a \frac{\cosh k(h + z_o)}{\sinh kh} \tag{3.33}$$

and

$$\hat{\zeta} = \frac{\hat{w}}{\omega} = a \frac{\sinh k(h + z_o)}{\sinh kh} \tag{3.34}$$

It can be seen from (3.31) and (3.32) that χ and ζ of any particle are 90° different in phase, and that the particle path during one wave cyle is an ellipse, with its major axis horizontal, with length $2\hat{\chi}$, and with its minor axis vertical, with length $2\hat{\zeta}$. A sketch is given in figure 3.3.

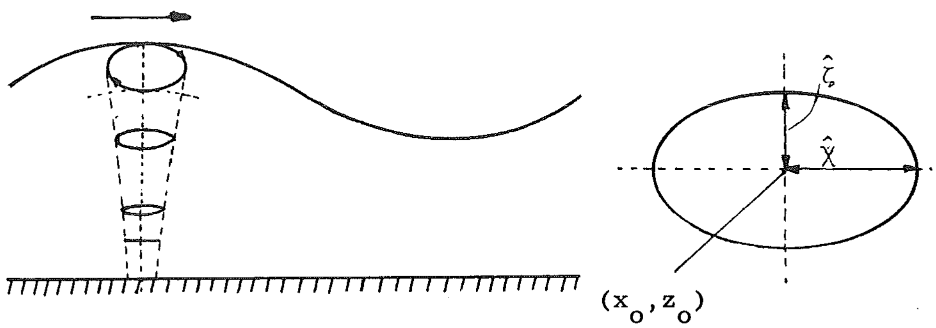

Figure 3.3

In the upper part of deep water, $\hat{u} = \hat{w}$, so that also $\hat{\chi} = \hat{\zeta}$, which means that the particle paths there are circular.

3.5. Dispersion equation, wavelength and phase velocity

The results derived in the paragraphs 3.2 through 3.4 are based on kinematic relations only. We will now introduce the dynamic surface condition (2.19). In doing so, we restrict ourselves to free waves. This determines a relation between wave frequency and wave number (ω and k), the so-called dispersion equation. Such equation is of central importance in the mathematical description of waves and vibrations. The form it takes in our case follows from the substitution of (3.7) and (3.10) into (2.19), which gives the dispersion equation for gravity surface waves (in the linear approximation):

$$\boxed{\omega^2 = gk \tanh kh} \tag{3.35}$$

At this stage we will revert to the use of wavelength ($L = 2\pi/k$) and waveperiod ($T = 2\pi/\omega$), which are used more in applications than wavenumber or frequency. Also, we introduce an auxiliary length, written as L_o, defined by

$$L_o \equiv \frac{gT^2}{2\pi} \tag{3.36}$$

Equation (3.35) can then be rewritten as

$$L = L_o \tanh \frac{2\pi h}{L} \tag{3.37}$$

It follows that in deep water, where $\tanh \frac{2\pi h}{L} \simeq 1$, the wavelength L equals L_o. In water of any depth, the quantity L_o is still defined, but it does not in general equal the local wavelength, which is a factor $\tanh 2\pi h/L$ smaller.

In order to facilitate the calculation of L for given h, g and T, (3.37) is written in dimensionless form:

$$\frac{h}{L_o} = \frac{h}{L} \tanh \frac{2\pi h}{L} \tag{3.38}$$

Values of h/L which are solutions of this equation for given h/L_o have been tabulated. Reference is made to Table 1.

The phase velocity c can be expressed in terms of wavenumber k or wavelength L by eliminating ω between (3.8) and (3.35), with the result

$$c = \left(\frac{g}{k} \tanh kh\right)^{\frac{1}{2}} = \left(\frac{gL}{2\pi} \tanh \frac{2\pi h}{L}\right)^{\frac{1}{2}} \tag{3.39}$$

Alternatively, we can eliminate k or L, with the result

$$c = \frac{g}{\omega} \tanh \left(\frac{\omega h}{c}\right) = \frac{gT}{2\pi} \tanh \left(\frac{2\pi h}{cT}\right) \tag{3.40}$$

By analogy with L_o, we can define a velocity c_o as

$$c_o \equiv \frac{gT}{2\pi} = \frac{L_o}{T} \tag{3.41}$$

after which (3.40) can be written as

$$c = c_o \tanh kh \tag{3.42}$$

It follows that in deep water

$$c = c_o = \frac{gT}{2\pi} = \frac{g}{\omega} = (\frac{gL_o}{2\pi})^{\frac{1}{2}} \quad (kh>>1) \tag{3.43}$$

By contrast, in shallow water (3.39) reduces to

$$c = (gh)^{\frac{1}{2}} \qquad (kh<<1) \tag{3.44}$$

which is the phase velocity of long waves of small amplitude.

Example

Given: $T = 8s$, $h = 10$ m, $a = 1$ m, $g = 9.8$ m s^{-2}

To be determined: L, c, $\hat{u}$ near MWL, $\hat{u}$ near bottom

Solution: $L_o = g\,T^2/(2\pi) = (1.56 \text{ m s}^{-2})T^2 \simeq 100$ m

$\rightarrow h/L_o = 0.1 \rightarrow$ Table $\rightarrow h/L = 0.141 \rightarrow L =$

$10 \text{ m}/0.1410 = 70.9$ m (alternative: Table $\rightarrow$

$\tanh kh = 0.709 \rightarrow L = L_o \tanh kh = 70.9$ m) $\rightarrow$

$c = L/T = 8.9 \text{ m/s}^{-1}$.

$\hat{u}\rfloor_{z=0} = \omega a/\tanh kh = (2\pi/8s)(1 \text{ m})/0.709 = 1.11 \text{ m s}^{-1}$.

$\hat{u}\rfloor_{z=-h} = \omega a/\sinh kh = (2\pi/8s)(1m)/1.006 = 0.78 \text{ m s}^{-1}$.

3.6. Pressure

Having determined the velocity potential, we can calculate the pressure from the Bernoulli equation (2.14). Neglecting the term $\frac{1}{2}(u^2 + w^2)$, this can be written as

$$p + \rho gz = -\rho\frac{\partial\phi}{\partial t} \tag{3.45}$$

In the absence of the waves, the pressure is denoted as p_o; it is hydrostatic:

$$p_o = -\rho gz \tag{3.46}$$

Denoting the wave-induced pressure by p_+, we have

$$p = p_o + p_+ \tag{3.47}$$

and therefore

$$p_+ = -\rho\frac{\partial\phi}{\partial t} \tag{3.48}$$

Substitution of (3.20) for $\emptyset$, and use of the dispersion equation (3.35), gives

$$p_+ = \hat{p}_+ \sin(\omega t - kx) \tag{3.49}$$

in which

$$\hat{p}_+ = \rho g a \frac{\cosh k(h+z)}{\cosh kh} \tag{3.50}$$

In deep water, (3.50) reduces to

$$\hat{p}_+ = \rho g a\, e^{kz} \qquad (kh>>1) \tag{3.51}$$

In shallow water it reduces to

$$\hat{p}_+ = \rho g a \qquad (kh<<1) \tag{3.52}$$

in which case (3.49) becomes

$$p_+ = \rho g \eta \qquad (kh<<1) \tag{3.53}$$

which is just a statement of hydrostatic pressure, a condition which is assumed a priori in theories for long waves.

A sketch showing the pressure distribution under a wave crest and under a wave trough is given in figure 3.4.

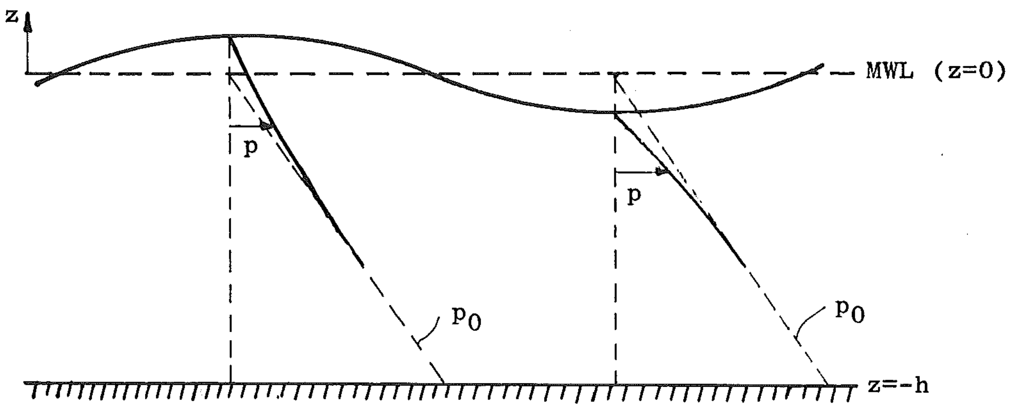

Figure 3.4

3.7. Energy content and energy transfer

An essential property of waves is their capacity of transferring energy from one region of space to another. Therefore, notions of energy content and energy transfer are important to an understanding of wave propagation.

In the preceding paragraphs, we considered the variations of characteristic properties of the wave motion with the vertical coordinate and with the phase. When dealing with energy, it is useful to consider the wave field in a more global or integral manner, by defining phase-averaged, vertically-integrated quantities. This is done for the energy content (E) as well as for the energy transfer rate (P).

The time-averaged, vertically-integrated kinetic energy of the waves per unit horizontal area is defined as

$$E_k \equiv \overline{\int_{-h}^{\eta} \frac{1}{2} \rho(u^2 + w^2)\, dz} \tag{3.54}$$

in which the overbar denotes a time-average. Substitution of (3.21) and (3.22) for u and w, and retaining only terms proportional to a^2 (so-called second-order terms), we find

$$E_k = \frac{1}{4} \rho(\omega a)^2 (k \tanh kh)^{-1} \tag{3.55}$$

This result is based on the kinematic part of the solution only; it is therefore valid regardless of the dynamic surface condition. However, if we restrict ourselves to free gravity surface waves, we can use the dispersion equation (3.35), in which case (3.55) can be written as

$$E_k = \frac{1}{4} \rho g a^2 \tag{3.56}$$

The time-averaged, vertically integrated potential energy of the waves per unit horizontal area is defined as

$$E_p \equiv \overline{\int_{-h}^{\eta} \rho g z dz} - \int_{-h}^{0} \rho g z dz = \frac{1}{2} \rho g \overline{\eta^2} \tag{3.57}$$

Substitution of (3.7) for η yields

$$E_p = \frac{1}{4} \rho g a^2 \tag{3.58}$$

Notice that $E_p = E_k$. This is no coincidence; it is a general property of free waves (in the linear approximation). Instead of following the route we have taken, we could have established (3.55) and (3.58) first, after which the dispersion equation would follow from equating E_k to E_p. This is Rayleigh's method, usually applied for calculating the natural frequencies of a vibrating system.

The total time-averaged, vertically integrated wave energy per unit horizontal area is defined as

$$E \equiv E_k + E_p \tag{3.59}$$

which gives

$$\boxed{E = \frac{1}{2}\rho g a^2 = \frac{1}{8}\rho g H^2} \tag{3.60}$$

The dimension of E_p, E_k and E is energy/area , or Jm^{-2} in the international system of units.

We next consider the energy <u>transfer</u> through a vertical plane of unit width, normal to the propagation direction (thus, x = const), which extends from bottom to surface. Water particles crossing this plane (at a velocity u) carry kinetic and potential energy with them ($\frac{1}{2}\rho(u^2 + w^2) + \rho gz$ per unit volume), and as they cross the plane the pressure (p) is doing work on them (at a rate pu per unit area). It follows that the rate at which energy is transferred across a unit area of the plane x = constant is given by

$$\{p + \rho gz + \frac{1}{2}\rho(u^2 + w^2)\}u \tag{3.61}$$

The time-averaged, vertically integrated energy transfer rate per unit width is now defined as

$$P \equiv \overline{\int_{-h}^{\eta} \{p + \rho gz + \frac{1}{2}\rho(u^2 + w^2)\}\, u\, dz} \tag{3.62}$$

Retaining only second-order terms, this can be approximated as

$$P = \int_{-h}^{0} \overline{p_+ \, u}\, dz \tag{3.63}$$

Substitution of (3.21) , (3.49) and (3.50) gives

$$\boxed{P = Enc} \tag{3.64}$$

in which, by definition,

$$n = \frac{1}{2} + \frac{kh}{\sinh 2\,kh} \qquad (\frac{1}{2} \leq n \leq 1) \tag{3.65}$$

In deep water, $n = \frac{1}{2}$, whereas in shallow water, n = 1 (see Table 1 as a function of kh).

The dimension of P is power/(crest)length, or Wm^{-1} in the international system of units.

Example (cont'd)

Data: see page 3.9.

To be determined: E and P.

Answer: $E = \frac{1}{2}\rho g a^2 = \frac{1}{2}(1035 \text{ kg m}^{-3})(9.8 \text{ ms}^{-2})(1 \text{ m})^2 = 5.1 \text{ kJ m}^{-2}$.

$h/L_o = 0.1 \rightarrow$ Table $\rightarrow n = 0.810 \rightarrow \quad nc = (0.810)(8.9 \text{ ms}^{-1})$

$= 7.2 \text{ ms}^{-1} \rightarrow P = Enc = (5.1 \text{ kJ m}^{-2})(7.2 \text{ ms}^{-1}) = 36.8 \text{ kJ s}^{-1} \text{ m}^{-1}$

$= 36.8 \text{ kW m}^{-1}$.

3.8. Wave trains and wave groups

The preceding results will now be used to calculate the velocity of propagation of a wave train, generated by a periodic disturbance some finite time ago, into a region of calm. The transition zone between the region of calm and the region of established wave motion is called the front of the wave train. We want to calculate its velocity, denoted as U_f (f for "front").

Consider the situation at two different times, $t = t_1$ and $t = t_1 + \Delta t$:

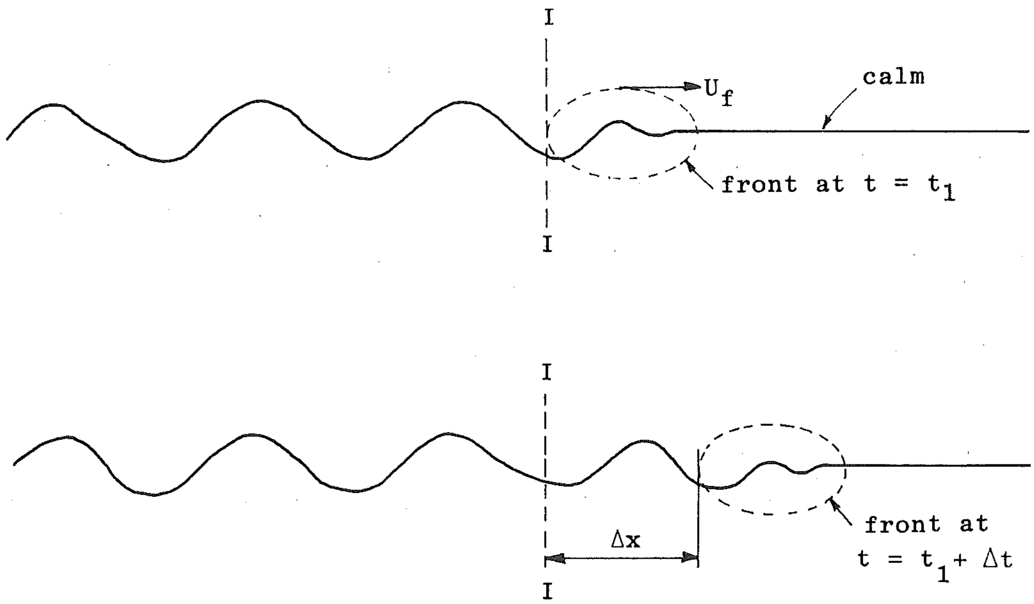

The region to the right of cross-section I-I contains more energy at $t = t_1 + \Delta t$ than at $t = t_1$, the gain being (per unit width):

$$E\Delta x = EU_f \Delta t \tag{3.66}$$

It has acquired this additional energy as a result of the energy transfer through the cross-section I-I in time Δt, which equals

$$P\ \Delta t \tag{3.67}$$

(per unit width). Equating the two gives

$$U_f = \frac{P}{E} \tag{3.68}$$

or, using (3.64) :

$$U_f = nc \tag{3.69}$$

The conclusion is that the wave front travels at a speed P/E, or nc, which in general differs from the phase velocity c. In deep water, nc equals $\frac{1}{2}$ c, or $gT/(4\pi)$. It is the velocity nc which should be used in calculating the arrival time at some location of waves from a distant disturbance (e.g. swell from a distant storm).

The fact that $U_f < c$ (except in shallow water) implies an advance of individual waves (wave crests) through the wave train, relative to the wave front. When such waves have arrived at the front, their amplitude goes to zero and they lose their identity.

So far, we considered the speed of propagation of a wave disturbance into a region of calm. However, the arguments and the results apply equally to a disturbance propagating into a region with a pre-existing wave motion. In other words, disturbances (modulations) of a wave field travel with the velocity nc. This applies also to the modulations in which the amplitude varies slowly between a maximum and a minimum (possibly zero), in which case we speak of <u>wave groups</u>.

A particular kind of wave groups is obtained by adding two periodic wave systems of slightly different frequency and wavenumber, traveling in the same direction:

$$\eta = \eta_1 + \eta_2 = a_1 \sin S_1 + a_2 \sin S_2 \tag{3.70}$$

with

$$S_1 = \omega_1 t - k_1 x\ ,\ S_2 = \omega_2 t - k_2 x \tag{3.71}$$

The phase difference between the two systems is

$$\delta S = S_2 - S_1 = (\delta\omega) t - (\delta k) x \tag{3.72}$$

in which

$$\delta\omega = \omega_2 - \omega_1 << \omega_1 \quad \text{and} \quad \delta k = k_2 - k_1 << k_1 \qquad (3.73)$$

Points of phase reinforcement (maximum amplitude) alternate with points of phase cancellation (minimum amplitude), as sketched in figure 3.5.

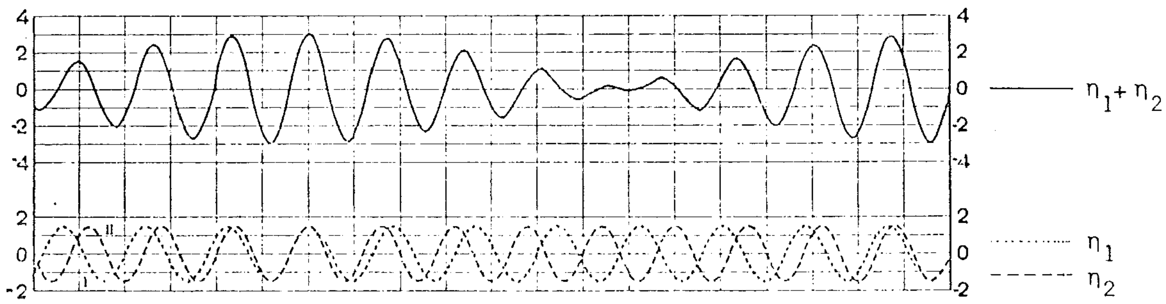

Figure 3.5 (source: Groen and Dorrestein, 1976)

The velocity of propagation of the groups, the so-called group velocity, denoted by c_g, can be calculated from the condition of constant phase difference between η_1 and η_2:

$$\frac{\partial}{\partial t}(\delta S) + c_g \frac{\partial}{\partial x}(\delta S) = 0 \qquad (3.74)$$

Using (3.72), this gives

$$c_g = \frac{\delta\omega}{\delta k} \simeq \frac{d\omega}{dk} \qquad (3.75)$$

Substitution of the dispersion equation (3.35) and carrying out the differentiation gives

$$c_g = nc \qquad (3.76)$$

in which the factor n is the same one as in (3.65). In other words, we see that the group velocity $d\omega/dk$, calculated on the basis of purely kinematic considerations (as above) has the same value as the propagation velocity P/E which was calculated on the basis of energy considerations. This is no coincidence: a wave group can be considered as an energy packet. The energy is where the group is, or vice versa. In what follows we will no longer make the distinction between the wave (front) propagation velocity and the group velocity, but use the name and symbol (c_g) of group velocity throughout. The equation for the energy transfer rate (3.64) is then written as

$$P = Ec_g \qquad (3.77)$$

3.9. Damping of waves by bottom resistance

In this paragraph, an estimate will be made of wave damping by bottom resistance. (Damping by bottom motion, or by percolation into a porous bottom, or by direct action of viscosity in the bulk of the water is usually less significant.)

Denoting the shear stress at the bottom by τ_b, and the particle velocity just outside the thin bottom boundary layer by u_b, we can express the average power dissipated per unit area (D) as

$$D = \overline{\tau_b u_b} \tag{3.78}$$

Assuming a turbulent boundary layer, we write

$$\tau_b = C_r \, \rho u_b \, | \, u_b \, | \tag{3.79}$$

in which C_r is a (dimensionless) resistance coefficient. It is a function of the ratio of particle displacement amplitude ($\hat{\chi}_b$) to bottom roughness, and of a boundary layer Reynolds number. A typical value of C_r for field conditions is 10^{-2}.

Substitution of (3.79) and (3.21) into (3.78) gives

$$D = \frac{4}{3\pi} C_r \, \rho \left(\frac{\omega a}{\sinh kh}\right)^3 \tag{3.80}$$

Having estimated the power dissipated per unit area, we now calculate the amplitude decay which is caused by that dissipation. To do that, we consider the energy contained in a volume of unit width, between two cross-sections $x = x_1$ and $x_2 = x_1 + \delta x$. The rates of energy transfer through these cross-sections are denoted by P_1 and P_2, where $P_2 \simeq P_1 + \frac{dP}{dx} \delta x$. The difference $(P_1 - P_2)$ is equal to the power dissipated over the length δx, which equals $D\delta x$ (per unit width), so that the energy balance becomes

$$\frac{dP}{dx} + D = 0 \tag{3.81}$$

Substitution of (3.80), (3.64) and (3.60) gives

$$\rho g n c a \frac{da}{dx} + \frac{4}{3\pi} C_r \, \rho \left(\frac{\omega a}{\sinh kh}\right)^3 = 0 \tag{3.82}$$

which can be written as

$$\frac{da}{a^2} + \beta dx = 0 \tag{3.83}$$

in which β is a (dimensional) constant given by

$$\beta = \frac{4}{3\pi} C_r \ (\omega/\sinh kh)^3/(gnc) \tag{3.84}$$

or, using (3.8) and (3.35), by

$$\beta = \frac{4}{3\pi} C_r \frac{k^2}{n(\sinh kh)^2 \ (\cosh kh)} \tag{3.85}$$

Finally, integration of (3.83) yields

$$\frac{1}{a(x)} = \frac{1}{a(x_1)} + \beta(x - x_1) \tag{3.86}$$

which indicates a hyperbolic decay of the amplitude with propagation distance. An alternative formulation of (3.86) is

$$\frac{a}{a_1} = (1 + \beta a_1 \ \Delta x)^{-1} \tag{3.87}$$

in which $a = a(x)$, $a_1 = a(x_1)$ and $\Delta x = x - x_1$. This shows that the relative decay rate depends not only on β, but also on the initial amplitude: higher waves are damped more rapidly (relative to the initial value) than lower waves. This is a consequence of the assumed quadratic bottom shear stress law (3.79).

The damping considered here is due to bottom resistance; the decay rate is therefore increasing with decreasing relative depth, as can also be verified by inspection of (3.85) ($\beta \to \frac{4}{3\pi} C_r h^{-2}$ as $kh \to 0$).

<u>Example</u> (cont'd)

Data: $T = 8$ s, $h = 10$ m (as above); $a_1 = 2$ m, $C_r = 10^{-2}$, $\Delta x = 3$ km
To be determined: a at $x_2 = x_1 + \Delta x$
Solution: $h/L_o = 0.1 \to$ Table $\to \sinh kh = 1.006$, $\cosh kh = 1.419$, $n_2 = .810$, $kh = .886 \to k = 0.0886 \ m^{-1} \to \beta = 2.9 \times 10^{-5} \ m^{-2} \to \beta a_1 \Delta X = 0.17 \to$ $a = 2 \ m/1.17 = 1.70$ m.

h/L_o	h/L	kh	$\tanh\ kh$	$\sinh\ kh$	$\cosh\ kh$	K_s	n
0	0	0	0	0	1	∞	1
.005	.02836	.1782	.1764	.1791	1.0159	1.692	.9896
.010	.04032	.2533	.2480	.2560	1.0322	1.435	.9792
.015	.04964	.3119	.3022	.3170	1.0490	1.307	.9690
.020	.05763	.3621	.3470	.3701	1.0663	1.226	.9588
.025	.06478	.4070	.3860	.4184	1.0840	1.168	.9488
.030	.07135	.4483	.4205	.4634	1.1021	1.125	.9388
.035	.07748	.4868	.4517	.5064	1.1209	1.092	.9289
.040	.08329	.5233	.4802	.5475	1.1401	1.064	.9192
.045	.08883	.5581	.5066	.5876	1.1599	1.042	.9095
.050	.09416	.5916	.5310	.6267	1.1802	1.023	.8999
.055	.09930	.6239	.5538	.6652	1.2011	1.007	.8905
.060	.1043	.6553	.5753	.7033	1.2225	.9932	.8811
.065	.1092	.6860	.5954	.7411	1.2447	.9815	.8719
.070	.1139	.7157	.6144	.7783	1.2672	.9713	.8627
.075	.1186	.7453	.6324	.8162	1.2908	.9624	.8537
.080	.1232	.7741	.6493	.8538	1.3149	.9548	.8448
.085	.1277	.8026	.6655	.8915	1.3397	.9481	.8360
.090	.1322	.8306	.6808	.9295	1.3653	.9422	.8273
.095	.1366	.8583	.6953	.9677	1.3917	.9371	.8187
.100	.1410	.8858	.7093	1.006	1.4187	.9327	.8103
.110	.1496	.9400	.7352	1.085	1.4752	.9257	.7937
.120	.1581	.9936	.7589	1.165	1.5356	.9204	.7776
.130	.1665	1.046	.7804	1.248	1.5990	.9169	.7621
.140	.1749	1.099	.8002	1.334	1.667	.9146	.7471
.150	.1833	1.152	.8183	1.424	1.740	.9133	.7325
.160	.1917	1.204	.8349	1.517	1.817	.9130	.7184
.170	.2000	1.257	.8501	1.614	1.899	.9134	.7050
.180	.2083	1.309	.8640	1.716	1.986	.9145	.6920
.190	.2167	1.362	.8767	1.823	2.079	.9161	.6796
.200	.2251	1.414	.8884	1.935	2.178	.9181	.6677
.210	.2336	1.468	.8991	2.055	2.285	.9205	.6563
.220	.2421	1.521	.9088	2.178	2.397	.9231	.6456
.230	.2506	1.575	.9178	2.311	2.518	.9261	.6353
.240	.2592	1.629	.9259	2.450	2.647	.9291	.6256
.250	.2679	1.683	.9332	2.599	2.784	.9323	.6164
.260	.2766	1.738	.9400	2.755	2.931	.9356	.6076
.270	.2854	1.793	.9461	2.921	3.088	.9390	.5994
.280	.2942	1.849	.9516	3.097	3.254	.9423	.5917
.290	.3031	1.905	.9567	3.284	3.433	.9456	.5845
.300	.3121	1.961	.9611	3.483	3.624	.9490	.5777
.320	.3302	2.075	.9690	3.919	4.045	.9553	.5655
.340	.3468	2.190	.9753	4.413	4.525	.9613	.5548
.360	.3672	2.307	.9804	4.974	5.072	.9667	.5457
.380	.3860	2.425	.9845	5.609	5.697	.9717	.5380
.400	.4050	2.544	.9877	6.329	6.407	.9761	.5314
.420	.4241	2.665	.9904	7.146	7.215	.9798	.5258
.440	.4434	2.786	.9924	8.075	8.136	.9832	.5212
.460	.4628	2.908	.9941	9.132	9.186	.9860	.5173
.480	.4822	3.030	.9953	10.32	10.37	.9885	.5142
.500	.5018	3.153	.9964	11.68	11.72	.9905	.5115

111. Table 1.

5. Diffraction of waves around breakwaters

5.1. Introduction

A wave train which meets an obstacle such as a breakwater or an offshore platform may be reflected backward and in lateral directions, but the wave crests can also bend around the obstacle and thus penetrate into the zone to the lee of the obstacle. This phenomenon is called diffraction. The degree of diffraction which occurs depends on the ratio of a characteristic lateral dimension of the obstacle (e.g. the length of a detached breakwater) to the wavelength.

For coastal and harbour engineers, the phenomenon of diffraction is important since it determines the shelter afforded by breakwaters and jetties. Sketches of the wave crest pattern are given below, for the diffraction around a detached breakwater and for the diffraction through a gap between two breakwaters. The reflected waves are omitted in these sketches.

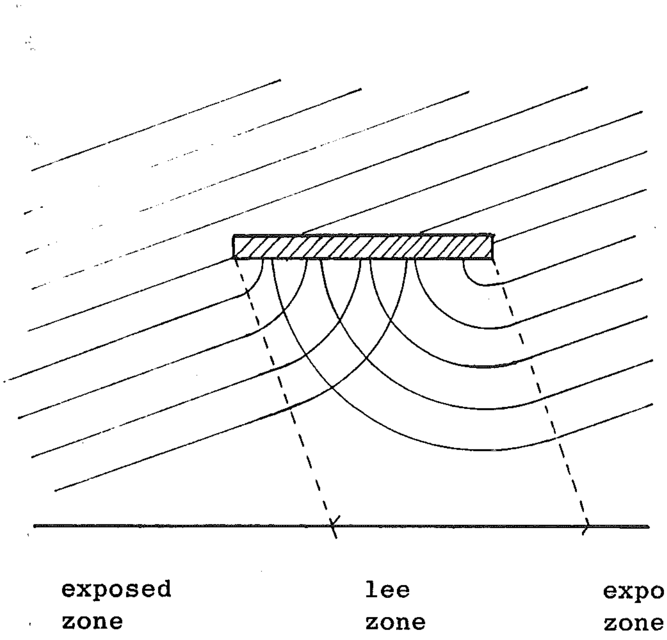

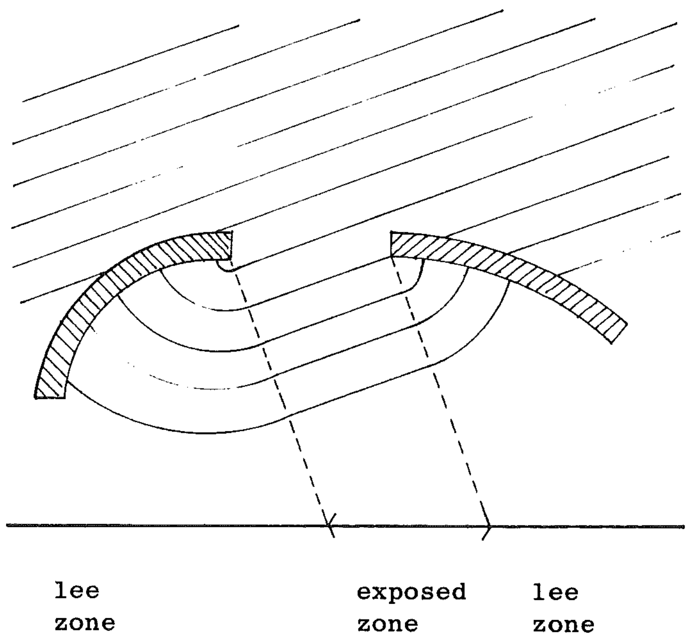

The mathematical theory of diffraction is outside the scope of this course. Only the assumptions and some results will be mentioned here, and a graphical approach to the problem of diffraction around breakwaters will be presented which can be applied in cases of relatively simple geometry, as sketched above. Cases of complicated geometry, particularly those involving multiple diffractions and reflections, require a scale model or a numerical mathematical model. These will not be dealt with here.

5.2. Assumptions

The assumptions made in the mathematical theory are the same as those used in the linear, potential-flow theory for free, two-dimensional, periodic, progressive gravity surface waves, with the exception of the two-dimensionality. In particular, it is stressed that the depth has been assumed constant. The obstacle around which the waves diffract is supposed to extend vertically from the bottom through the free surface, and to be rigid and impermeable (which implies that it is fully reflecting).

The assumptions listed above allow a solution for the velocity potential in the form

$$\phi(x,y,z,t) = \frac{\omega a(x,y)}{k} \frac{\cosh k(h+z)}{\sinh kh} \cos\{\omega t-\Psi(x,y)\} \tag{5.1}$$

with an associated surface elevation given by

$$\eta(x,y,t)= a(x,y) \sin\{\omega t-\Psi(x,y)\} \tag{5.2}$$

The frequency ω and the wavenumber k obey the dispersion equation (3.35).

The amplitude $a(x,y)$ and the phase $\Psi(x,y)$ are unknown functions, to be determined from the governing equations and the boundary conditions specifying the incident waves (usually long-crested, constant amplitude) and the shape, size and orientation of the obstacle (in plan view). The mathematical solution can be visualized by plots of isolines of $a(x,y)$ and $\Psi(x,y)$. The former are usually presented in dimensionless form, by plotting isolines of the so-called diffraction factor K_D:

$$K_D(x,y) = \frac{a(x,y)}{a_\infty} \tag{5.3}$$

in which a_∞ is the amplitude of the incident waves where these are not disturbed by the obstacle. Plots of isolines of $\Psi(x,y)$ give the crest pattern, since a wave crest is the locus of points which at any instant have the same phase.

Analytical diffraction solutions are available only for obstacles with a highly idealized geometry, such as an elliptical or circular cylinder, or a semi-infinite, straight screen. In the latter case, the presence of the screen (or breakwater) can be expressed by the boundary condition

$$v = \frac{\partial\phi}{\partial Y} = 0 \text{ at } X>0\text{ , } Y = 0 \tag{5.4}$$

where (X,Y) are coordinates along the breakwater and normal to it. Eq. (5.4)

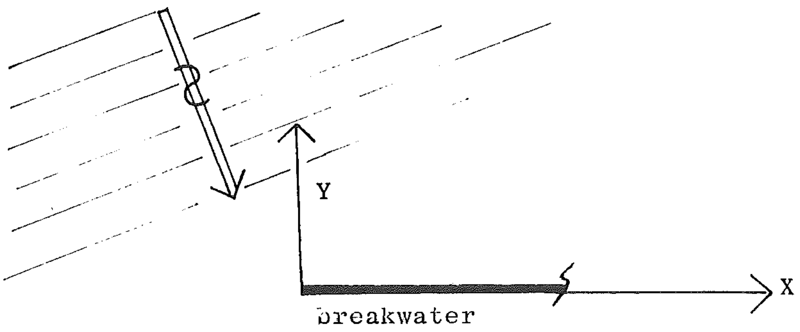

implies that in the mathematical model the screen or breakwater is of zero thickness, straight, semi-infinite in extent, rigid and impermeable. The applicability of the results for this idealized representation to diffraction around real breakwaters will be discussed later (paragraph 5.7).

The solution to the problem of diffraction of a uniform wave train around a breakwater represented by (5.4) was first given by Sommerfeld. A graphiccal presentation of his solution will be given in the following paragraphs, after a brief discussion of the effects of reflection.

5.3. Influence of reflection

The solution derived by Sommerfeld consists of the sum of two terms, which can be considered as the diffracted, incident wave field and the diffracted, reflected wave field, as sketched below:

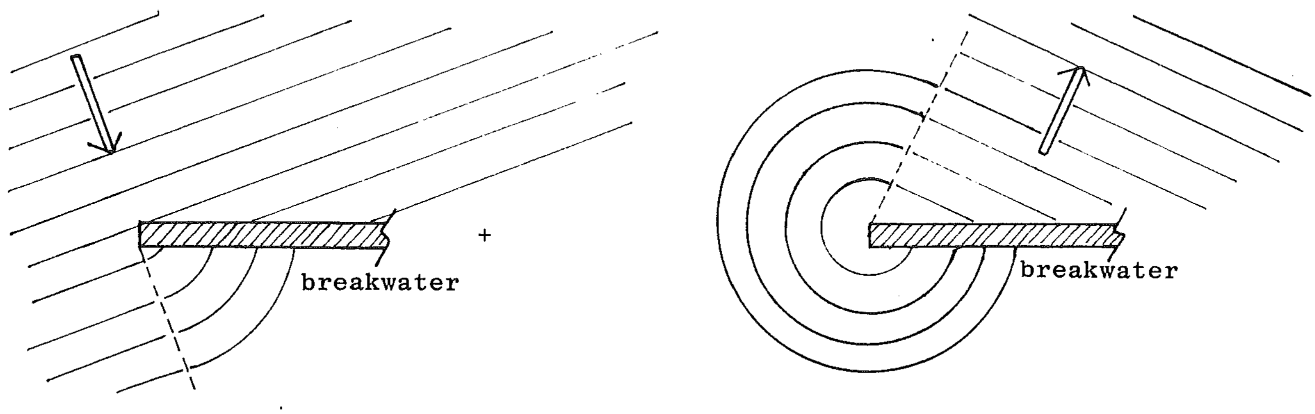

An inspection of the two parts of the Sommerfeld solution shows the following points:

. The diffraction of the incident waves and that of the reflected waves are mathematically expressed by the same function, the so-called Fresnel integral.

The amplitude of the diffracted, reflected waves is relatively small on the lee side of the breakwater (except very near the breakwater itself).

The first of these two points suggests that the diffraction of an abruptly cut-off wave system has a universal pattern. If so, it is sufficient to consider only the diffracted incident waves to study that pattern. The second point implies that this gives a good approximation to the actual solution in the region on the lee side of the breakwater.

For the reasons indicated above, only the diffraction of the incident wave field will be considered in what follows, with neglect of the reflection. A graphical procedure will be described with which this part of the solution can be obtained. It is pointed out that the same graphical procedure can be applied to the reflected waves if this is considered necessary in order to obtain the complete solution. If the breakwater is only partially reflecting, the second part can be multiplied with an appropriate reduction factor (the reflection coefficient) before it is added to the first part, representing the incident waves. (Note: the isolines of K_D given in the Shore Protection Manual (CERC, 1975) are based on the complete Sommerfeld solution, i.e. with 100% reflection.)

5.4. Huygens' principle

The graphical presentation of the Sommerfeld solution can be explained qualitatively by using Huygens' principle, according to which an advancing wave front can be considered as a sequence of elementary wave sources, each of which radiates energy in a circular pattern.

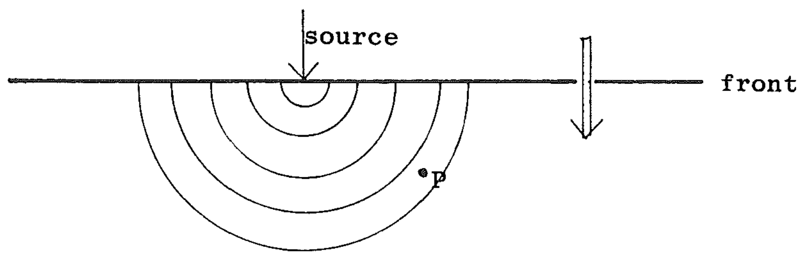

The wave disturbance at some point P can be determined by adding the contributions from the various sources which can reach it. If this summation is carried out over all the sources from $-\infty$ to $+\infty$, the undisturbed, incident wave motion is recovered. If a breakwater is present, the summation is carried out only over those sources which can reach P by wave rays, i.e. by straight lines if the depth is constant. This explains why and how Huygens' principle can be used in diffraction studies.

5.5. Cornu spiral

It appears from the above that it is necessary to construct graphically the resultant of a large number of sinusoidally varying quantities, as in

$$\eta_p(t) = \sum_j a_j \cos(\omega t + \Psi_j) \tag{5.5}$$

in which the index j indicates the number of an elementary source.

At time t=0, (5.5) reduces to

$$\eta_p(0) = \sum_j a_j \cos \Psi_j \tag{5.6}$$

The quantity $a_1 \cos \Psi_1$ can be represented as the projection, on a reference axis, of a vector with length a_1, enclosing an angle Ψ_1 with the reference axis:

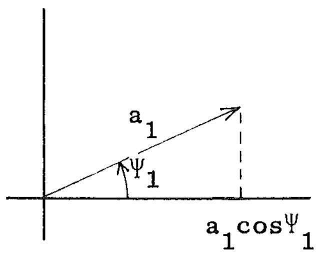

The same holds for $a_2 \cos \Psi_2$. The sum $(a_1 \cos \Psi_1 + a_2 \cos \Psi_2)$ can be obtained from the resultant of the two vectors, which

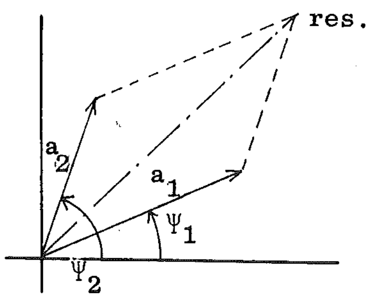

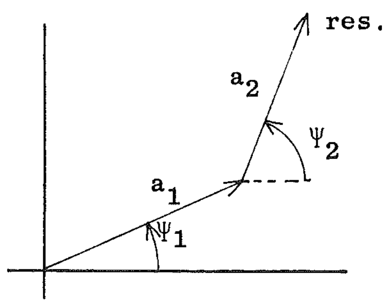

in turn can be obtained conveniently by drawing the second vector from the end point of the first one, as shown in the sketch on the right. This can be extended to any number of vectors. The result for t≠0 can be obtained by rotating all vectors through an angle ωt. This operation need not be carried out; it is sufficient to realize that it <u>can</u> be done, and that the length of the resultant vector represents the amplitude of the sum in (5.5).

We now return to the case of a straight incident wave front approaching a point P. In absence of any obstacle, the situation is symmetric about the normal on the front through P. The wave front is divided into sources of equal strength, numbered j=1,2,3,.... to the right of the projection (P') of P on the front, and j=-1,-2,-3,.... to the left of P'.

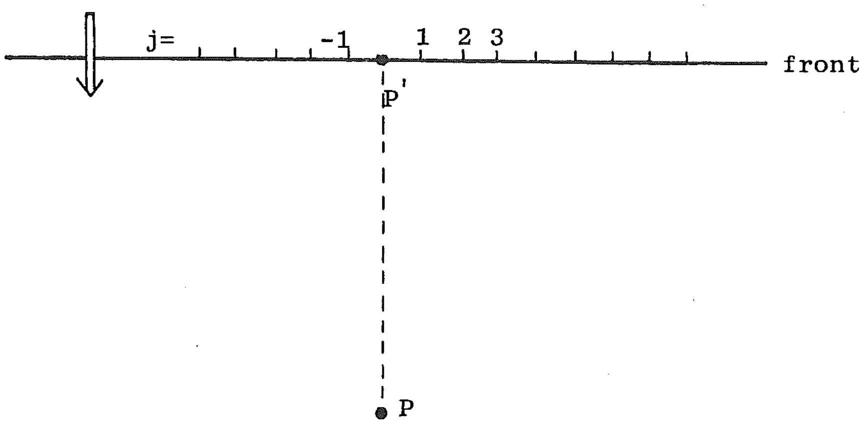

Let the contribution of source 1 to $\eta_P(t)$ be represented by a vector. Source 2 is at a greater distance from P, so that its contribution to $\eta_P(t)$ will lag in phase behind the contribution from source 1, and have a smaller amplitude. The vector representing the second contribution is therefore rotated clockwise with respect to the vector from source 1, and it is shorter. Continuing in this fashion to the right of P', (to j=+∞), a sequence of vectors is obtained of monotonically decreasing length, rotated clockwise with respect to the previous one. In this

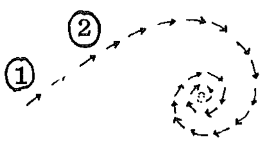

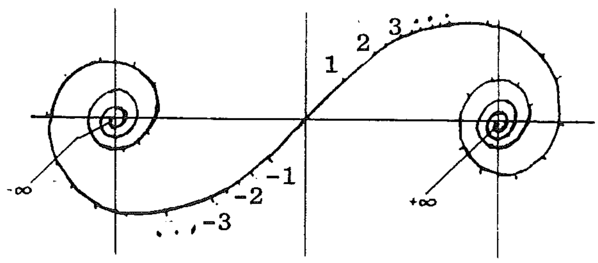

manner a spiral is formed (a smooth curve in the limit of infinitesimal source dimensions), whose limit point corresponds to the sources at +∞. The contributions from the sources to the left of P' (to j = -∞) are obtained by simply adding the mirror image of the spiral about the point corresponding to P'. The result is called the Cornu spiral.

The sum of the contributions from all the sources (from $-\infty$ to $+\infty$) gives the undisturbed, incident wave, with respect to amplitude (a_∞) as well as phase. In the Cornu spiral, this is represented by the vector drawn from the limit point "$-\infty$" to the limit point "$+\infty$". The length of this vector represents a_∞, and its orientation represents the phase of the incident wave at P.

It can be seen that through the procedure described above, the incident wave front, extending from $-\infty$ to $+\infty$, is mapped onto the spiral, with a one-to-one correspondence between (point) sources on the front, as "seen" from P, and their images on the spiral. This correspondence can be formulated quantitatively as follows.

Let Q be an arbitrary point on the incident wave front, at a known distance r_Q from P. Its image on the Cornu spiral for point P can be determined from the phase difference between the contributions to η_P from the sources at P' and at Q, which is

$$\Delta\Psi_{P'Q} = 2\pi \, \frac{r_Q - y}{L} \tag{5.7}$$

in which y is the distance (P' P). This phase difference equals the angle enclosed between the tangents to the Cornu spiral in the images of P' and Q, denoted by $\tilde{P}'$ and $\tilde{Q}$. Thus, knowing r_Q, y and L, $\Delta\Psi_{P'Q}$ can be calculated from

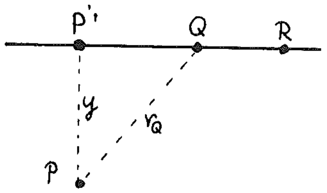

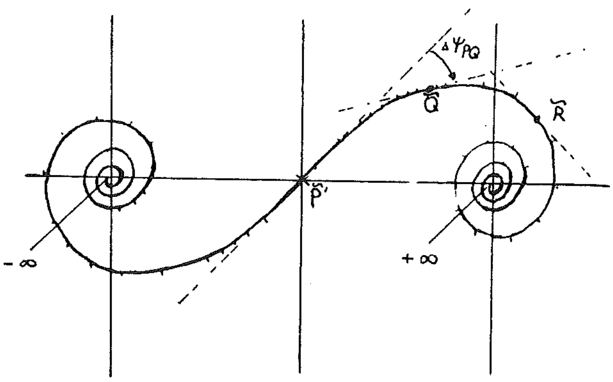

(5.7), and this determines uniquely the point $\tilde{Q}$ on the spiral, knowing that it must be between $\tilde{P}'$ and the limit point "$+\infty$" (see sketch).

In practice, it is more convenient to work with fractions of cycles, given by (r-y)/L, than with angles. For this reason, a parameter W is used, defined by

$$W = \frac{r-y}{L} \tag{5.8}$$

Values of W have been plotted along the copy of the Cornu spiral provided with these lecture notes. (To avoid cluttering of the figure, points with equal decimal value of W have been connected by dashed curves.) To give an example, consider a point R such that $r_R - y = \frac{1}{4}$ L, or $W_R = \frac{1}{4}$. This means that $\Delta\Psi_{P'R} = \pi/2$, and that $\tilde{R}$ is the first point on the spiral between $\tilde{P}'$ and "+∞" where the tangent to the spiral is normal to that at $\tilde{P}$. It can be located as the point where W = 0.25.

5.6. Application to single breakwater

The preceding results will now be applied to determine the wave amplitude in a point near a single breakwater around which diffraction occurs, as sketched below

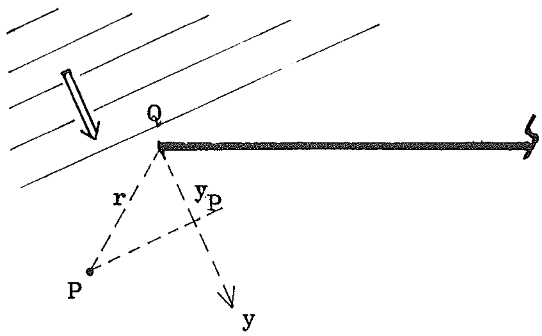

(1) A y- coordinate is defined in the direction of propagation, with its origin (y=0) in the breakwaterhead Q.

(2) The value of W = (r-y)/L is calculated, where r is the radial distance from Q to the point P considered, and y is the y- coordinate of P.

(3) The image ($\tilde{Q}$) of Q on the Cornu spiral is determined, using the value of W calculated in (2), taking care that $\tilde{Q}$ is in the proper half of the spiral (in the example shown, between $\tilde{P}_1$ and "+∞").

(4) The vector sum is determined of the contributions from all those sources of the incident wave front which can reach P via straight lines (which can be "seen" from P). In the example given, it is the vector drawn from the limit point "-∞" to $\tilde{Q}$. The length of that vector represents the wave amplitude at P, to a scale determined by the fact that the distance between the two limit points represents a_∞.

Example

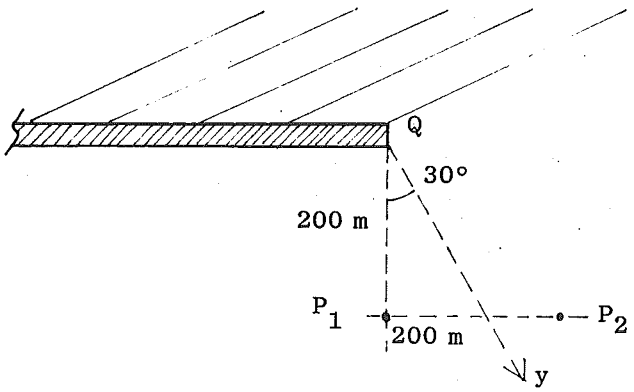

$\alpha_\infty = 30°$, $L = 100$ m,
$a_\infty = 3$ m

$a_{P_1} = ?$ $a_{P_2} = ?$

P_1: $r = 200$ m
$y = (200 \text{ m})(\cos 30°) = 174$ m
$\Big\} \; W = \frac{r-y}{L} = 0.26$

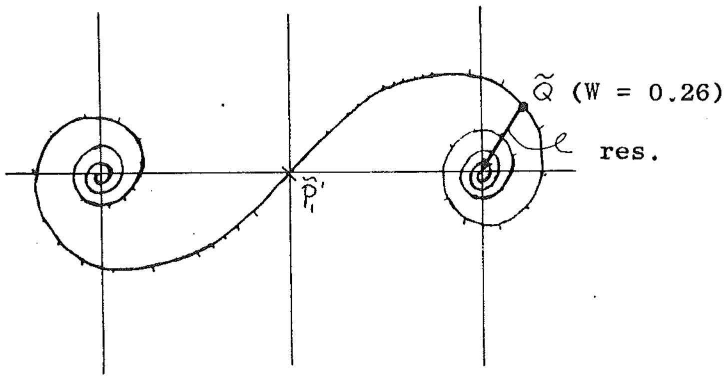

Resultant = vector from $\tilde{Q}$ to "+∞", with length 39 mm. Distance between limit points is 198 mm, which represents $a_\infty = 3$ m. Thus:

$$a_{P_1} = \frac{39}{198}(3 \text{ m}) = 0.58 \text{ m}$$

P_2: $r = (200 \text{ m})\sqrt{2} = 283$ m
$y = (200 \text{ m})(\cos 30° + \sin 30°) = 274$ m
$\Big\} \; W = \frac{r-y}{L} = 0.09$

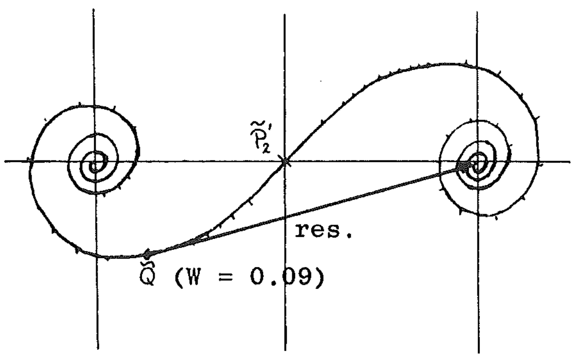

Resultant = vector from $\tilde{Q}$ to "+∞", with length 175 mm. Thus,

$$a_{P_2} = \frac{174}{198}(3 \text{ m}) = 2.61 \text{ m}$$

Note that the image of the breakwaterhead on the spiral depends on the point of observation (P_1 or P_2).

If the procedure described above is repeated for all points on a line across the line separating the lee zone from the exposed zone (the so-called shadow line), the following picture emerges:

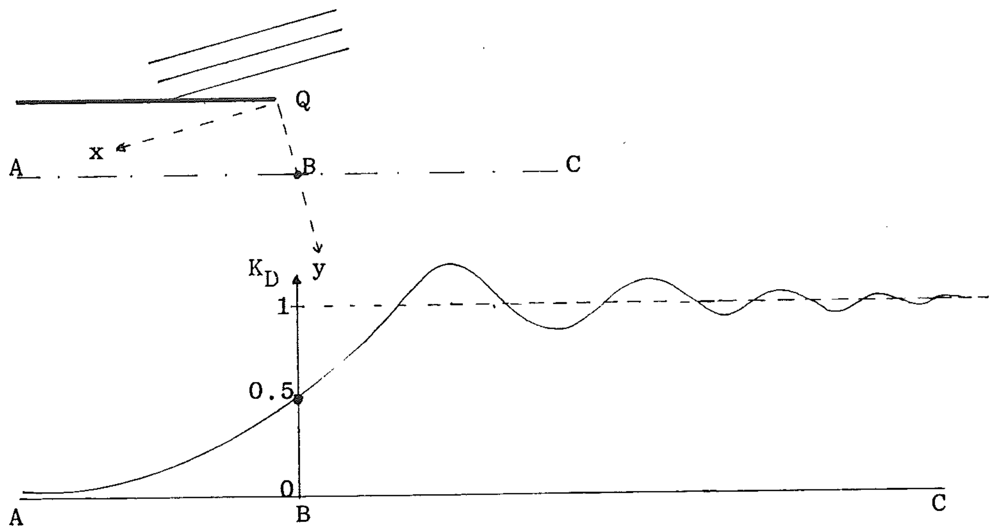

Instead of a discontinuity in wave amplitude, which would exist if diffraction did not occur (K_D = 0 along AB, K_D = 1 along BC), we see a smooth transition, with a value K_D = 0.5 along the shadowline. Inside the shadow zone the amplitude decreases monotonically with increasing distance from the shadow line, and in the exposed zone it oscillates increasingly rapidly but with decreasing amount around the value 1. The first and largest maximum of K_D is approximately 1.17; it occurs for $W \simeq 0.36$. This value of W (or any other) occurs not in one point only, but in a locus of points which can be determined by noting that $r = WL+y$, or

$$x^2 = (WL)^2 + 2\,WL\,y \tag{5.9}$$

which is the equation of a parabola if W = const. The

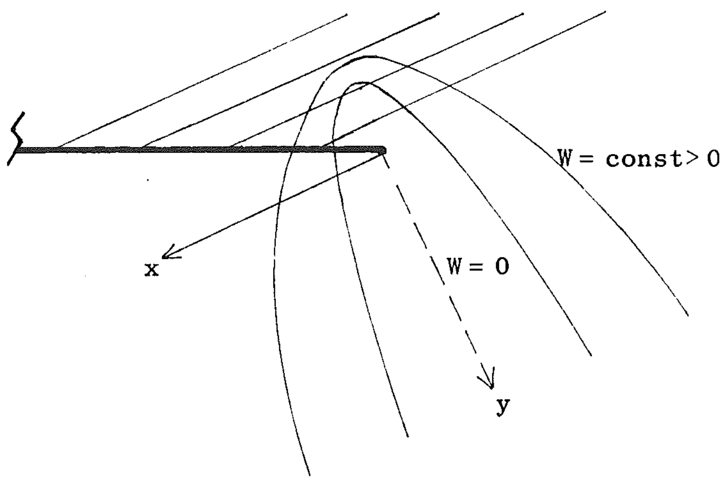

shadow line, where W = 0, is a reduced parabola.

For completeness' sake, it is repeated that the procedure described above can also be applied to the waves which are reflected off the breakwater. The resultant vector, possibly reduced in length to allow for partial reflection, can be added to the one representing the diffracted incident waves, after rotating it through a certain angle so as to achieve that both resultants have the same reference phase angle. The details of that operation are not described here.

5.7. Generalizations

The Sommerfeld theory of diffraction has been derived on a certain set of assumptions, listed in paragraph 5.2. In this paragraph we shall review the assumptions pertaining to the breakwater, and point out how these can be relaxed so as to widen the field of practical applications.

The thickness of the screen, or the width of the breakwater, is theoretically zero. Practically, it is sufficient if it is small relative to the wave-length. Within that finite width, the sides need not be vertical.

The reflection was assumed to be 100% in the theory, but since its influence is relatively small anyway in the zone away from the area which is directly exposed to the reflected waves, this condition can be dropped. In fact, in the procedure described in the preceding paragraph, the reflection is neglected entirely, and this approximation is better as the actual reflection coefficient is smaller.

The breakwater is theoretically rigid. This is a fairly realistic assumption for conventional breakwater structures such as those of the caisson-type or rubble-mound breakwaters. Needless to say, the Sommerfeld theory cannot be applied to compliant breakwaters (e.g. of the floating type) since these transmit wave energy to the lee zone by their own motion. A similar statement applies to the permeability.

Finally, we consider the geometry of the breakwater in plan view. Theoretically, it is a semi-infinite, straight line. However, in the approximation given above, in which the effect of reflection is neglected, the value of K_D in a point is determined exclusively by the value of W, and by the fact whether the point is inside or outside the shadow zone. The orientation of the breakwater relative to the incident waves does not affect K_D. In this approximation, the diffraction is purely an edge effect (using a terminology from diffraction of light waves around the edge of a screen). In other words, the approximation described in paragraph 5.6 would apply to the diffraction of a uniform incident wave field which is somehow cut off abruptly. This makes it plausible that the breakwater which causes the cut-off need not be straight, or infinite in extent. In fact, diffraction around more than one breakwaterhead can be described by the above method, applied to each head separately, provided it is still a reasonable approximation that each breakwaterhead is approached by a more or less uniform wave train. This is the case if each breakwaterhead is in the exposed zone, sufficiently far away (say a few wavelengths or more) from the shadow lines through the other breakwaterheads.

Examples of diffraction around more than one breakwaterhead have been given in the sketch in paragraph 5.1, showing a breakwater gap and a detached breakwater. The calculation of the diffraction through a gap will be illustrated in the following.

Example

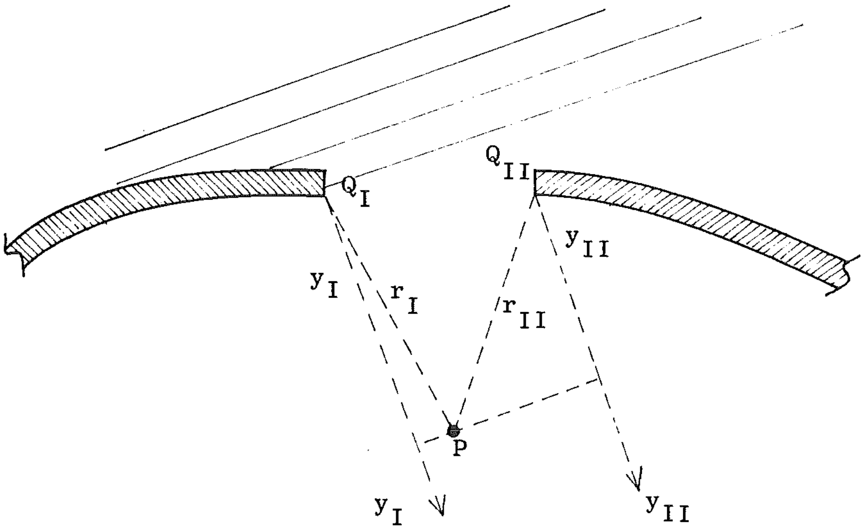

From known breakwater geometry, incident wave direction and wavelength, and location of P, calculate

$$W_I = \frac{r_I - y_I}{L} \text{ and } W_2 = \frac{r_{II} - y_{II}}{L}$$

Say (for example) that $W_I = 0.25$ and $W_{II} = 0.40$.

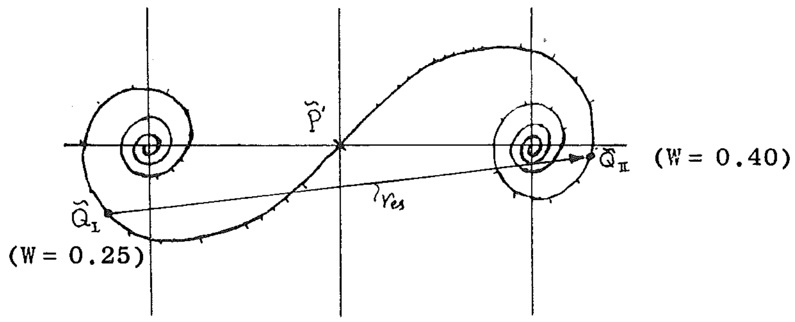

Resultant of sources reaching P = vector from $\tilde{Q}_I$ to $\tilde{Q}_{II}$, which appears to have a length of 255 mm, so that $K_D = 255/198 = 1.28$.

Note that in case of diffraction through a gap, there is one point in which K_D is greater than anywhere else. It is determined by the longest vector connecting two points of the Cornu spiral. It occurs for $W_I = W_{II} \simeq 0.39$, (i.e., at the intersection of two parabolas of $W \simeq 0.39$, one for each breakwaterhead), and the corresponding $K_D = K_{D\ max} \simeq 1.34$.

4. Nonlinear theories for waves in constant depth

4.1. Introduction

No exact solution to the equations presented in chapter 2 has been found which would represent periodic, irrotational waves of permanent form. This is due to the nonlinear terms in the free surface boundary conditions. In the linear approximation, these nonlinear terms were neglected entirely. In nonlinear theories, they are taken into account by approximation. Numerous nonlinear theories have been developed, with different methods and different degrees of approximation. In this chapter, a brief, mainly qualitative overview of these is presented.

A nonlinear theory for irrotational water waves was first developed by Stokes (1847). His theory, to be dealt with in par. 4.2 below, is in principle applicable to waves in water of arbitrary depth relative to the wavelength, but it turns out that for shallow-water waves the results are realistic only if the wave height is exceedingly small.

A second category of theories has been developed especially for shallow-water conditions. These will be considered in paragraph 4.3.

The theories referred to above give explicit, analytical expressions for the various coefficients needed in the formulation. The so-called numerical theories give algorithms to evaluate the coefficients numerically for any given specific set of input conditions. A few of these numerical theories will be mentioned in par. 4.4.

The question of the validity of the various theories is taken up in par. 4.5.

4.2. Stokes theory

Stokes (1847) employed a method of successive approximations, which can roughly be described as follows.

The results of the linear theory are used to find a first approximation to the neglected nonlinear terms. Taking these into account, corrections to the first (linear) approximation of the solution are determined.

With these corrected approximations of the exact solution, a second approximation of the nonlinear terms can be made, etc. If this process converges, it can in principle be continued until the corrections become sufficiently small. (A practical limit is soon reached because the mathematical expressions become very lengthy as higher-order approximations are worked out.)

A typical linear term is proportional to a cos S or a sin S, in which "a" is the amplitude of the surface elevation in the linear approximation, and $S = \omega t - kx$ is the phase. Since the nonlinear terms consist of product terms such as u^2, the first approximation to these terms consists of terms proportional to $a^2 \cos^2 S = \frac{1}{2} a^2 (1 + \cos^2 S)$, and similar terms with sin S. The same is true of the first correction to the linear approximation of the exact solution. Continuing in this manner, one finds successive approximations to the exact solution in the form of successive terms of a power series in "a" (terms proportional to a, a^2, a^3, etc.). If "a" is sufficiently small (relative to L and h), each higher-order term will be small compared to the lower-order terms, and if then the series is terminated after a few terms, a useful approximation may have been obtained.

As mentioned above, the mathematical expressions occurring in the high-order approximations become quite lengthly. Application of the theory has been made easier by the preparation of graphs and tables, such as those of Skjelbreia (1959) for the 3rd order approximation, in which all terms of order 3 and less retained and all others are neglected.

In the following, some of the results will be mentioned, mainly in a qualitative sense.A few equations of the second order theory will be presented for purposes of illustration.

Surface profile. The 2nd-order expression for the surface elevation can be written as

$$\eta(S) = \hat{\eta}_1 \cos S + \hat{\eta}_2 \cos S \qquad (4.1)$$

in which

$$\hat{\eta}_1 = a \qquad (4.2)$$

$$\hat{\eta}_2 = \tfrac{1}{4} ka^2 \frac{(\cosh kh)(2 + \cosh 2kh)}{(\sinh kh)^3} \qquad (4.3)$$

The reference point S=0 has been chosen in a wave crest. A sketch of (4.1) is given in figure 4.1.

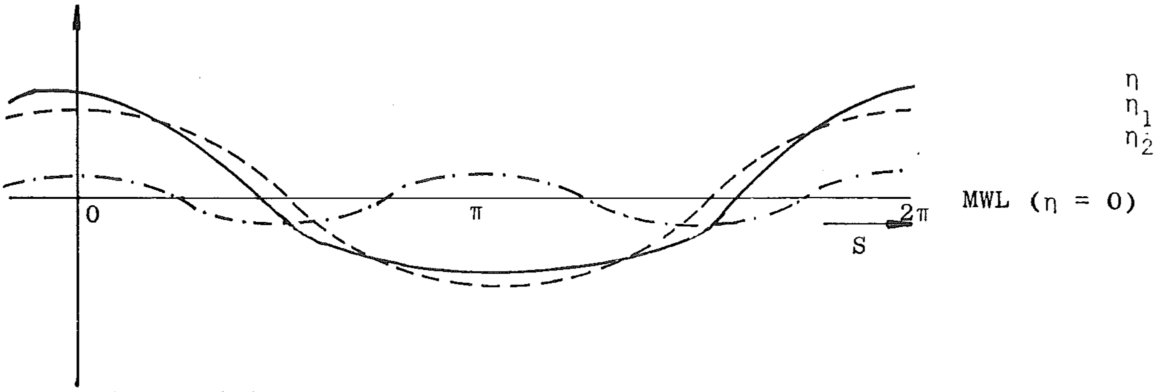

Figure 4.1.

The profile appears to have crests which are narrower and more peaked than those of a cosine-profile, and ughs which are broader and flatter. Consequently, the elevation of the wave crests is more than one half of the waveheight above MWL, the excess being given by $\hat{\eta}_2$ (to second order). This is important for the calculation of wave forces on structures in shallow water, or for the determination of the required clearance between the deck of a platform above the design MWL (the so-called "air-gap").

The asymmetry noted above can clearly be observed in real water waves. The measured profiles appear to be very well predicted by the Stokes 2nd- or 3rd-order theory in case of deep-water waves, but the agreement gets worse for the more shallow-water conditions. An indication for this can be obtained from the theory itself, particularly from the ratio of 2nd-order amplitude to 1st-order amplitude, which should be small for the Stokes approach to be valid. In deep water, this ratio is (see eqs. 4.2 and 4.3)

$$\frac{\hat{\eta}_2}{\hat{\eta}_1} \cong \tfrac{1}{2} ka \cong \frac{\pi}{2} \frac{H}{L} \; (kh>>1) \qquad (4.4)$$

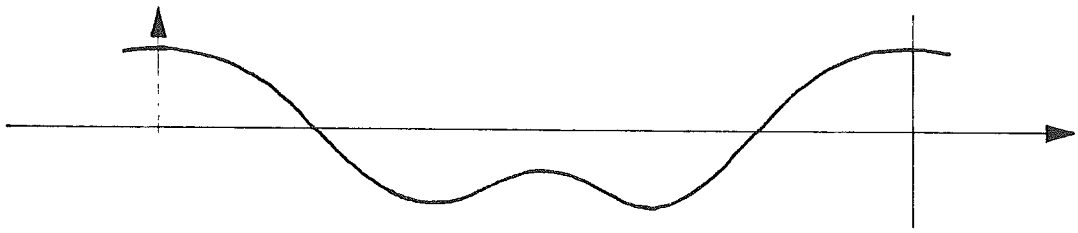

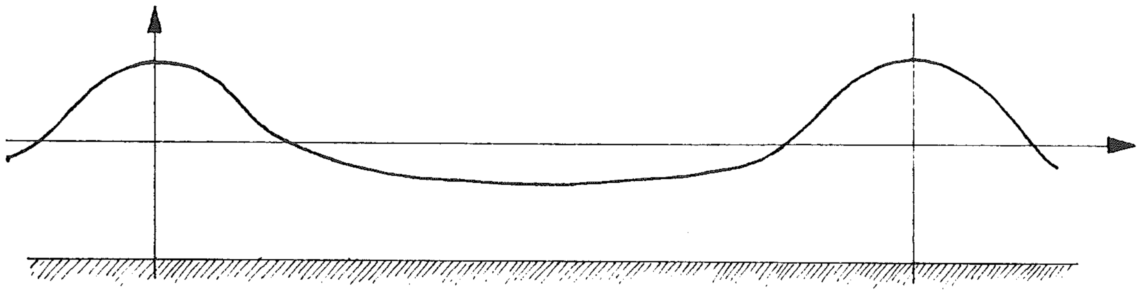

which is always small (approximately 0.2 at most), because breaking limits the possible steepness of the waves. By contrast, in shallow water said ratio becomes (see eqs. 4.2 and 4.3)

$$\frac{\hat{\eta}_2}{\hat{\eta}_1} \cong \frac{3}{4}\,(kh)^{-3}\,(ka) \cong \frac{3}{32\pi^2}\,\frac{HL^2}{h^3} \cong 10^{-2}\,\frac{HL^2}{h^3} \quad (kh<<1) \qquad (4.5)$$

If we require $\hat{\eta}_2 \lesssim 0.2\hat{\eta}_1$ then the following inequality must hold:

$$\frac{HL^2}{h^3} \lesssim 20 \qquad (4.6)$$

This is a very strict requirement on H/L since L>>h in shallow water. The ratio HL^2/h^3 is often called the Ursell number, denoted by U:

$$U \equiv \frac{HL^2}{h^3} \qquad (4.7)$$

If U is too large then the Stokes series diverges. One indication of this is the appearance of a secondary maximum in the wave trough, as sketched below:

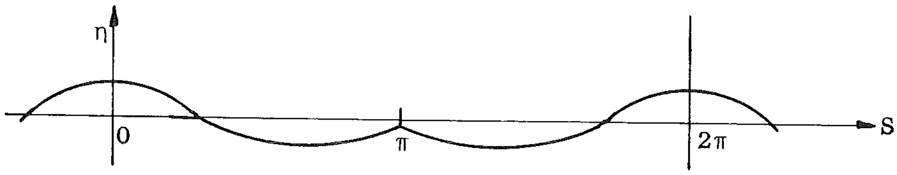

This is not observed in waves of permanent form. If it occurs in the theory (which is the case if $\hat{\eta}_2 > \hat{\eta}_1/4$), it is an indication that the theory is used outside the limits of its applicability.

Measurements of high waves of permanent form in shallow water show profiles with long, flat troughs and narrow, peaked crests:

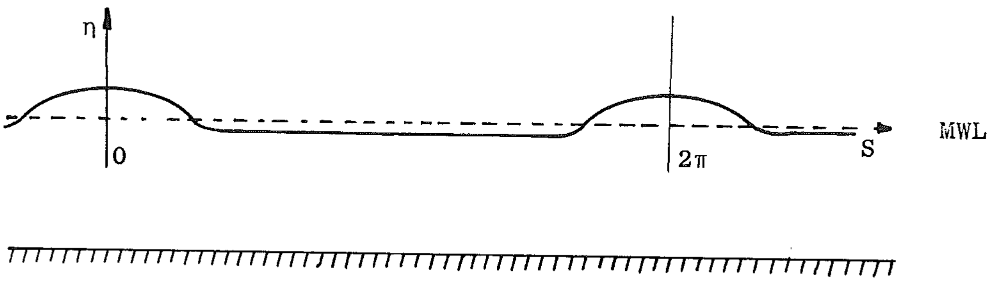

If such profile is to be represented as a sum of harmonic cos-terms (cos S, cos 2S etc.) then many such terms would be required. This means that the series would have to be evaluated to very high order. Therefore, the Stokes series would be impractical for these conditions anyway, even if it did not diverge.

Particle velocities. In the nonlinear approximation, the particle velocities are no longer symmetric about their mean value (which is zero below the level of the wave troughs, in the reference system chosen here). The horizontal velocities have an asymmetry which is qualitatively similar to that of the surface elevation. Thus, the velocity has greater absolute value under the crest than under the trough. This can have a significant influence on the calculated wave forces on piles, particularly in shallow-water conditions. The higher-order terms in the series for the particle velocities decrease more rapidly with distance below the surface than the lower-order terms. Near-bottom velocities are fairly well predicted by linear theory.

Particle paths. In the linear theory, particle paths were calculated on the assumption that the differences in velocity of the particle itself and that in its mean position could be neglected. This led to a particle path which was symmetric about the vertical axis and about the horizontal axis. In nonlinear theories, said differences are not entirely neglected. The result is a particle path which is no longer symmetric. The upper part is more strongly curved than the lower part, and - which is more significant - the particle path is no longer closed, but after one wave period the particle will have experienced a net forward advance, as sketched below:

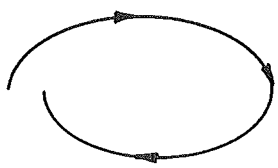

Thus, the waves cause a net mass transport (relative to our reference system. Alternatively, we could have chosen a reference system such that the net, vertically integrated mass transport would be zero. In that case, the particles in the lower part of the vertical profile would have a backward net velocity, and only those in the upper part a forward net velocity.). To the 2nd order, the time-averaged velocity of a particle of mean elevation z_o, for deep-water conditions, is given by

$$\bar{u}\ (z_o) = (ka)\ (\omega a)\ e^{2kz_o} \qquad (kh \gg 1) \qquad (4.8)$$

In intermediate depths and in shallow water, the Stokes prediction of the mass transport velocities is not realistic, which is due to the influence of viscosity. (Note that viscous effects are restricted to a thin boundary layer only as far as the oscillatory part of the flow is concerned.) A re-analysis of the mass transport in water waves, including effects of viscosity, has been given by Longuet-Higgins (1953).

Energy content and energy transfer. In the lowest order of approximation the energy content (E) and energy transfer rate are proportional to a^2. The nonlinear corrections to this consist of terms proportional to a^4, a^6, etc. The total energy of waves of a given height turns out to be less than that predicted by the linear theory. This can be seen without mathematical calculations for the average potential energy, which is equal to $\frac{1}{2}\rho g \overline{\eta^2}$. The ratio $\overline{\eta^2}/H^2$ decreases as the profile becomes more spiky.

In deep water, the nonlinear corrections to E and P are significant only for almost-breaking waves. They are more important in shallow water, but in that case the Stokes series is not suitable except for very small relative wave heights, as discussed above.

Dispersion equation and phasevelocity. In the 2nd-order Stokes approximation, the dispersion equation is the same as in the linear theory. In the 3rd-order, a nonlinear correction term appears, proportional to the square of the wave steepness; its effect is to increase the phase velocity, which therefore in any depth becomes not only frequency-dependent but also amplitude-dependent. Although the correction is relatively small (usually a few % only), it can be significant when differences in phase velocity are relevant, as is the case in wave groups.

4.3. Cnoidal theory

An approach to nonlinear waves in shallow water has been developed by Boussinesq. The so-called Boussinesq equations describe waves in shallow water, with some allowance for non-hydrostatic pressure, as would occur under the crests, where the curvature is relatively strong even if the wavelength is much larger than the depth. Thus, solutions to the Boussinesq equations have some long-wave properties and some short-wave properties as well.

The solutions of the Boussinesq equations representing periodic waves of permanent form are described by means of a mathematical function with the symbol "cn", for which reason such solutions are called "cnoidal waves", and the corresponding theory is called the "cnoidal theory". Actually, different approaches and different degrees of approximation have been developed for cnoidal waves, so that we cannot speak of "the" cnoidal theory. In what follows, we mention some results of the approximation used by Skovgaard et al. (1974) for the preparation of tables. (Note: participants in this course are required to have a copy of these tables.)

Before dealing with specifics, two general remarks are made. First, the cnoidal theory is by its very nature restricted to shallow-water conditions, for which the criterion $h/L_o \lesssim 0.1$ (or $T\ (g/h)^{\frac{1}{2}} \gtrsim 8$) is adopted. Second, an important parameter in the theory is the Ursell number ($U = HL^2/h^3$, see eq. 4.7). The cnoidal-type of mathematical functions describing the solution for arbitrary value of U reduce to simpler forms in the two limiting cases $U \to 0$ and $U \to \infty$. The first of these corresponds to $H/h \to 0$ (since $L/h >> 1$ in the cnoidal theory). The results in this case reduce to those of the linear theory for shallow water. The second limiting case corresponds to $L/h \to \infty$ (since H/h is finite; in fact, it has been assumed that $H/h << 1$). This gives rise to so-called solitary waves.

Surface profile. The shape of the surface profile as predicted by the cnoidal theory depends on U only (see fig. 1 of Skovgaard et al. 1974). For $U \to 0$ it is sinusoidal, as expected (see above). With increasing value of U, the crests become narrower and more peaked, and the troughs become longer and flatter. Values of η_{min}/H have been tabulated as a function of U, from which the relative crest elevation η_{max}/H can be determined. Predicted profiles generally agree fairly well with measured profiles.

Particle velocities. In the 1st-order cnoidal theory, the horizontal particle velocity is roughly proportional to the surface elevation in the same vertical, and it varies with distance from the bottom as a second-degree parabola. Reference is made to Skovgaard et al. (1974) for formulae for u_{max} and u_{min}.

Phase velocity. The phase velocity in the cnoidal theory is in order - of - magnitude given by $(gh)^{\frac{1}{2}}$, with a slight decrease due to the restricted value of the ratio of wavelength to waterdepth (a frequency-dependent effect, as in the linear theory for short waves) and a slight increase due to the finite amplitude (a nonlinear effect).

Potential energy and energy transfer. The average potential energy per unit area (E_p, eq. 3.57) is proportional to $\overline{\eta^2}$. For a sinusoidal profile, $\overline{\eta^2} = H^2/8$. For a cnoidal profile, whose shape depends on U, the ratio $B \equiv \overline{\eta^2}/H^2$ is a decreasing function of U. It has been tabulated by Skovgaard et al. (1974).

To the lowest order of approximation, the energy transfer rate in a cnoidal wave is calculated from (3.63), with p_+ given simply by the hydrostatic approximation $p_+ = \rho g \eta$, and u by the linear long-wave expression $u = c\eta/h$. This gives

$$P \cong \int_{-h}^{o} \overline{p_+ u}\, dz \cong \rho g c \overline{\eta^2} = B\, \rho g H^2 c \tag{4.9}$$

Actually, p_+ is not hydrostatic, and it is in absolute value less than $\rho g \eta$ at points below MWL. Therefore, (4.9) overestimates the energy transfer rate. We shall return to this later.

4.4. Numerical theories

The theories referred to above yield analytical expressions for the coefficients appearing in the assumed power series for the various dependent variables, to the order of approximation considered. The complexity of these expressions increases rapidly with increasing order, for which reason high-order analytical approximations are not feasible. It is however possible to develop algorithms to evaluate the coefficients numerically. In this manner, one can go to very high order (e.g. 100) so as to extend the range of applicability of the theory and to increase the accuracy. Theories in which this is done are called "numerical theories". (Note that this name does not imply a numerical solution of the basic differential equation, e.g. by finite-difference methods or by finite element methods.)

A well-known numerical theory is the so-called streamfunction theory developed by Dean (1965). Its use has been made relatively easy by the preparation and publication of tables (Dean, 1974). These tables have been made for engineering applications. Among others, they contain data for phase velocity, particle velocities and accelerations, and wave forces and moments on vertical cylinders. These quantities have been tabulated for 10 relative depths (h/L_o in the range from 0.02 to 2) and 4 relative wave heights ($H/H_{max} = \frac{1}{4}, \frac{1}{2}, \frac{3}{4}$ and 1, in which H_{max} is the maximum height of a wave of permanent form of given length or period in a given waterdepth, as discussed in par. 4.5).

Chaplin (1980) has developed an alternative version of the streamfunction theory which gives greater accuracy for the very steep waves. He compared his results and those given by Dean (1974) with the virtually exact theory by Cokelet (see below). Dean's tabulated values were confirmed for the lower three values of H/H_{max}, but for $H/H_{max} = 1$ significant deviations were found (e.g., 30% error in maximum particle velocity).

A different numerical theory has been given by Cokelet (1977), who used recurrence relations between coefficients of different order so as to extend the solution to very high order. In addition, Cokelet used certain mathematical techniques to improve the summation of the resulting series. In so doing he was able to calculate various wave properties to an accuracy of several decimal places, even for the highest possible waves, as was verified by comparison with independently developed theories for this special case. It appears that from a practical point of view, Cokelet's work can be regarded as giving a virtually exact solution to the classical problem of periodic, nonlinear, irrotational surface gravity waves of permanent form. If nothing else, his results can be used as a standard of comparison for various more approximate theories. Cokelet has presented tables of certain phase-independent and average wave properties, but not of instantaneous values such as particle velocities and accelerations, so that use of his theory in engineering applications will generally require that a (fairly complex) computer program be written.

4.5. Regions of validity

Before taking up the question of the validity of the various nonlinear theories, the region in which periodic waves of permanent form can exist is discussed.

With increasing wave steepness (H/L), the ratio u_{max}/c increases, where u_{max} is the particle velocity at the wave crest. It can reach the value 1, which is generally taken to be the limiting condition for waves of permanent form. The crests become angular in this limit, with an angle of

120°. The corresponding limiting steepness is a function of the relative depth (h/L). The following approximate expression for this relationship has been derived by Miche (1944):

$$\left(\frac{H}{L}\right)_{max} \cong 0.14 \tanh \frac{2\pi h}{L} \qquad (4.10)$$

In deep water this reduces to

$$\left(\frac{H}{L}\right)_{max} \cong 0.14 \qquad (kh \gg 1) \qquad (4.11)$$

In this limiting case, the wavelength L is about 10% larger than it is in the linear approximation $(gT^2/(2\pi)$.

In shallow water, (4.10) reduces to

$$\left(\frac{H}{h}\right)_{max} \cong 0.89 \qquad (kh \ll 1) \qquad (4.12)$$

The region in the (h/L, H/L)-plane corresponding to values of H/L not exceeding $(H/L)_{max}$ is the region in which waves of permanent form are possible. Attempts have been made in the past to delineate certain sub-regions in which certain approximate solutions would be most valid. The following points are noted in this respect:

. From an academic point of view, a delineation of regions of validity of approximations is hardly relevant after Cokelet presented a virtually exact solution.

. There is no unique answer to the question which approximation, of any given set of approximations considered, is most nearly valid for a given combination of H/L and h/L. The answer depends on the parameters used in the comparison (phase velocity, maximum crest elevation, etc.).

. From a practical point of view, the decision to use one or another approximation depends not only on the accuracy which can be achieved, but also on the accuracy which is needed, and the effort which can be made. In this connection, it is noted that there is little point in aiming at an accuracy of a few %, if the input conditions can be in error by 10% or 20%.

It is clear from the above that there is no such thing as "the best" theory or approximation for a given (H/L, h/L). Therefore, at most a few general guidelines can be given:

. If only theories are considered with published tables, then the choice is virtually restricted to the linear theory, the Stokes 3rd-order approximation, the cnoidal 1st-order approximation, and Dean's stream function theory (the latter only for $H/H_{max} \geq \frac{1}{4}$).

- Of these, Dean's theory is most widely applicable.
- A higher-order approximation is not necessarily better than a lower-order one, because the series used may be divergent. For instance, for large values of the Ursell number, the 1st-order Stokes theory (linear theory) gives a better approximation of particle velocities than does the 2nd-order or 3rd-order Stokes approximation. The same is true for cnoidal theories.
- Nonlinearities are relatively more important for local values (e.g. crest elevation, maximum particle velocities) than for overall properties (phase velocity, average energy content, etc.).
- The relative magnitude of nonlinear terms decreases with increasing distance below the free surface.

CHAPTER 26

SURF SIMILARITY

J.A. Battjes
Civil Engineering Department
Delft University of Technology
Netherlands

ABSTRACT

This paper deals with the following aspects of periodic water waves breaking on a plane slope: breaking criterion, breaker type, phase difference across the surfzone, breaker height-to-depth ratio, run-up and set-up, and reflection. It is shown that these are approximately governed by a single similarity parameter only, embodying both the effects of slope angle and incident wave steepness. Various physical interpretations of this similarity parameter are given, while its role is discussed in general terms from the viewpoint of model-prototype similarity.

FLOW PARAMETERS

Consider a rigid, plane, impermeable slope extending to deep water or to water of constant depth from which periodic, long-crested waves are approaching. The wave crests are assumed to be parallel to the depth contours.

The motion will be assumed to be determined wholly by the slope angle α, the still water depth d and the incident wave height H at the toe of the slope, the wave period T, the acceleration of gravity g, the viscosity μ and the mass density ρ of the water; g, μ and ρ are assumed to be constants. Effects of surface tension and compressibility are ignored.

Let X be any dimensionless dependent variable, then

$$X = f(\alpha, \frac{H}{L_0}, \frac{d}{L_0}, Re) \qquad (1)$$

in which Re is a typical Reynolds number, and

$$L_0 = \frac{gT^2}{2\pi} , \qquad (2)$$

i.e. the deep-water wavelength of small-amplitude sinusoidal, longcrested gravity surface waves with period T. The ratio H/L_0 is a wave steepness, if we define this parameter in a generalized sense as the ratio of a wave height to a wave length.

Variations in the flow regime are brought about mainly by variations of α and H/L_0, for the Reynolds number is usually larger than some minimum value above which variations in its actual value do not significantly affect the resultant motion, while for waves breaking on the slope, the value of the relative depth in front of the slope is not important either; this is well established for the relative run-up [7] and the reflection coefficient [14], for instance. So, in summary one can say that for waves breaking on the slope (1) reduces to

$$X \approx f(\alpha, \frac{H}{L_0}) , \qquad (3)$$

while it will be shown in the following that for many overall-properties of the breaking waves (3) reduces further to

$$X \approx f(\xi) , \qquad (4)$$

in which ξ is a similarity parameter, defined by

$$\xi = \frac{\tan \alpha}{(H/L_0)^{\frac{1}{2}}} . \qquad (5)$$

To the author's knowledge, this parameter was first used by Iribarren and Nogales [8], for determining whether wave breaking would occur. Its more general usefulness in the context of surf problems was suggested by Bowen et al [3].

FLOW CHARACTERISTICS DETERMINED BY THE SIMILARITY PARAMETER ξ

Breaking criterion

Iribarren and Nogales [8] have given an expression for the condition at which the transition occurs between non-breaking and breaking of waves approaching a slope which is plane in the neighbourhood of the still-water line. They use the shallow-water trochoidal theory for uniform, progressive waves. According to this theory, progressive waves are at the limit of stability if their amplitude ($\frac{1}{2}H$) equals the mean depth (d). Thus, denoting the condition of incipient breaking by the index "c",

$$\tfrac{1}{2}H_c = d_c \tag{6}$$

The depth d_c at which this would occur is equated by Iribarren and Nogales to the mean undisturbed depth in the one-quarter wavelength adjacent to the still-water line, or

$$d_c = \frac{1}{2}\left(\frac{1}{4} L_c \tan\alpha_c\right) = \frac{1}{8} L_c \tan\alpha_c \quad . \tag{7}$$

The wavelength L_c is calculated as $T_c\sqrt{gd_c}$, so that

$$d_c = \frac{1}{8} T_c \sqrt{gd_c} \tan \ {}_c \quad . \tag{8}$$

Elimination of d_c between (6) and (8) gives

$$(T\sqrt{g/H}\tan\alpha)_c = 4\sqrt{2} \tag{9}$$

or, substituting (2) and rearranging,

$$\xi_c = \left(\frac{\tan\alpha}{\sqrt{H/L_0}}\right)_c = \frac{4}{\sqrt{\pi}} \approx 2.3 \quad . \tag{10}$$

Laboratory experiments by Iribarren and Nogales and others [8, 13] have confirmed the validity of (10), with the proviso that $\xi \approx 2.3$ corresponds to a regime about halfway between complete reflection and complete breaking. This quantitative agreement is considered to be fortuitous because one can raise valid objections against the derivations on several scores. These pertain to the numerical estimates used by Iribarren and Nogales, rather than to the approach as such. For instance, the limiting height for waves in shallow water is given by (6) as twice the depth, which is unrealistic. A height-to-depth ratio of order one seems more reasonable. The author has elsewhere [1] suggested more realistic values for the various numerical factors in (6), (7) and (8), which however happened to yield exactly the criterion (9) again. Even so, the fact that (9) is correct not only qualitatively but also quantitatively is still

considered to be somewhat fortuitous, because derivations such as these can be useful for indicating the form in which the respective variables are to be combined, but they cannot in general be expected to give correct quantitative predictions.

The derivation given by Iribarren and Nogales suggests a physical interpretation of the parameter ξ, at least if wave breaking occurs ($\xi < \xi_c$). Consider the local steepness of the breaking waves. Their celerity is proportional to $(gd)^{\frac{1}{2}}$, their wavelength to $T(gd)^{\frac{1}{2}}$, and their steepness to $H/(T(gd)^{\frac{1}{2}})$, or to $(H/gT^2)^{\frac{1}{2}}$, since H/d is of order one for waves breaking in shallow water. Thus, the parameter ξ, given by

$$\xi \equiv \frac{\tan\alpha}{\sqrt{H/L_0}} = \frac{1}{\sqrt{2\pi}}\,\frac{\tan\alpha}{\sqrt{H/gT^2}} \quad , \tag{11}$$

is roughly proportional to the ratio of the tangent of the slope angle (the slope "steepness") to the local steepness of the breaking wave. The criterion for breaking given by Iribarren and Nogales can therefore be said to imply that incipient breaking corresponds to a critical value of this ratio.

Breaker types

So far the parameter ξ has been considered only in the context of a breaking criterion, that is, as an aid in answering the question whether wave breaking will occur. However, it also gives an indication of how the waves break. The main types are surging, collapsing, plunging and spilling breakers [9, 15, 4]. These occur in the order of increasing wave steepness and/or decreasing slope angle. The transition from one breaker type to another is of course gradual. The values of α and H/L_0 mentioned in what follows should be considered as indicating the order of magnitude only of the values in the transition ranges.

Galvin [4] has presented criteria regarding breaker types in terms of an "offshore parameter" $H_0/(L_0 \tan^2\alpha)$, in which H_0 is a deep-water wave height calculated from the motion of the generator bulkhead and the water depth, and an "inshore parameter" $H_b/(gT^2 \tan\alpha)$. The index "b" refers to values at the break point, which is taken to be the most seaward location where some point of the wave front is vertical, or, if this does not occur, the location where foam first appears at the crest.

Galvin's offshore parameter can be written as ξ_0^{-2}, in which the index "0" refers to deep water (wave height). Converting the critical values of the offshore parameter given by Galvin to values of ξ_0 gives

surging or collapsing	if	$\xi_0 > 3.3$
plunging	if	$0.5 < \xi_0 < 3.3$
spilling	if	$\xi_0 < 0.5$

These results are based on experiments on slopes of 1:5, 1:10 and 1:20.

The inshore parameter used by Galvin, $H_b/(gT^2 \tan\alpha)$, is not equivalent to the parameter ξ_b used here. However, a re-analysis of Galvin's data in terms of $\xi_b = (H_b/L_0)^{-\frac{1}{2}} \tan\alpha$ showed that the classification of breakers as plunging or spilling could be performed equally well with ξ_b as with Galvin's inshore parameter [1]. The following approximate transition values were found:

surging or collapsing	if	$\xi_b > 2.0$
plunging	if	$0.4 < \xi_b < 2.0$
spilling	if	$\xi_b < 0.4$

The possibility of using a parameter equivalent to ξ_b as a breaker type discriminator has also been noted by Galvin in a more recent review of breaker characteristics [5].

Phase difference across the surfzone

Not only the form of a breaking wave varies with ξ, but the distance of the break point from the mean water line as well. This distance, expressed in wave-lengths, is estimated at roughly $(d_b \cot\alpha)/(\frac{1}{2}T\sqrt{gd_b}) \approx 0.8\ \xi_b^{-1}$, where we have put $H_b \approx d_b$. Observations by the author on slopes between 1:3 and 1:25, with ξ-values from 0.15 to 1.9, have indicated that his estimate is qualitatively correct, but that it is roughly 20% too high. With spilling breakers there are at least two breaking or broken waves in the surf zone simultaneously. This number ranges from zero to two for plunging breakers. Collapsing breakers occur almost at the instantaneous water's edge, so that there is at most one of these present at any one time. Reference should be made in this connection to Kemp [10], who points out that the total phase difference across the surf zone is indicative of the type of wave motion, and of the corresponding equilibrium profile

of sand or shingle beaches.

Breaker height-to-depth ratio

The ratio of wave height to water depth at breaking is an important parameter of the surf zone; it is here denoted by the symbol γ_b:

$$\gamma_b = \frac{H_b}{d_b} \qquad (12)$$

The depth d_b is here defined as the still-water depth at the break point.

Values of γ_b generally range between 0.7 and 1.2. Bowen et al [3] suggest that γ_b may be a function of ξ_o only. The data presented by them are given in fig. 1. In addition, data have been plotted from Iversen [9], from Goda [6], and from unpublished results obtained by the present author.
It can be observed that the results from Bowen et al [3] form a separate group, outside the range of the others. The reason for this is not known. The other points in fig. 1 show a weak trend with ξ_0. For values of ξ_0 less than about 0.2, in the range of spilling breakers, they are scattered about a value of $\gamma_b \approx 0.8$, while there is a slow increase with ξ_o for higher values.

The scatter in the results may partly be due to the fact that for this purpose the independent variables H/L_0 and α cannot adequately be combined in the single parameter ξ. However, even the values of γ_b presented by various authors for the same values of α and H/L_0 show considerable scatter. This is undoubtedly to some extent due to the difficulties and ambiguities inherent in defining (experimentally) and measuring breaker characteristics. Another factor contributing to the scatter may be the occurrence of parasitic higher-harmonic free waves which are often inadvertently generated along with the intended wave train. The secondary waves affect the breaking process in a manner depending on the phase difference with the primary wave, which in turn depends (among others) on the distance from the wave generator. This distance is not commonly introduced as an independent variable, so that any effects which it may have on the results can appear as unexplained scatter.

Set-up, run-up and run-down

The set-up is defined as the wave-induced height of the mean level of the water surface above the undisturbed water level. Theoretical and experimental results [11, 3] indicate that the gradient of the set-up in the surf zone on gently sloping beaches is proportional to the beach slope; the coefficient of proportionality is a function of γ, the average height-depth ratio of the waves in the surf zone. The maximum set-up is roughly equal to $0.3\ \gamma\ H_b$.

The run-up height R_u is defined as the maximum elevation of the waterline above the undisturbed water level. A simple and reliable empirical formula for the run-up height of waves breaking on a smooth slope has been given by Hunt [7]. It can be written as

$$\frac{R_u}{H} = \xi \qquad \text{for } 0.1 < \xi < 2.3 \tag{13}$$

An investigation by Battjes and Roos [2] of some details of the run-up of breaking waves on dike slopes (1:3, 1:5, 1:7), such as the mean velocity of advance, particle velocities, layer thickness and so on, has shown that many of these parameters are functions of ξ only if normalized in terms of the incident wave characteristics.

Measurements of the run-down height R_d (minimum elevation of the waterline above the undisturbed water level) are very scarce, and, if available, not very accurate since run-down is rather ill-defined experimentally. An analysis of the measurements by Battjes and Roos [2], supplemented with unpublished data gathered for this study, has indicated that in the experimental range ($\cot \alpha = 3,5,7,10$; $0.02 < H/L_0 < 0.09$; $0.3 < \xi < 1.9$) the run-down height R_d is roughly equal to $(1 - 0.4\ \xi)R_u$. In other words, the ratio of the variable part of the vertical motion of the waterline $(R_u - R_d)$ to the maximum elevation above S.W.L. is approximately $0.4\ \xi$. It has a maximum value of about 1 for waves in the transition from non-breaking to breaking, and decreases with decreasing ξ. For very small ξ the set-up constitutes the greater part of the run-up height.

Reflection and absorption

The relative amount of wave energy that can be reflected off a slope is intimately dependent on the breaking processes and the attendant energy dissipation. Because of this, and in view of the fact that these processes appear to be governed to such a large extent by the parameter ξ, it is natural to try to relate the reflection coefficient to ξ.

The reflection coefficient r is defined as the ratio of the amplitude of the reflected wave to the amplitude of the incident wave. The estimation of r on a slope generally takes place according to a procedure given by Miche [13] who assumes that the reflected wave height equals the maximum height possible for a non-breaking wave of the given period on the given slope; in other words, only the energy corresponding to the height in excess of the critical height is assumed to be dissipated. This gives

$$\begin{aligned} r_{th} &= \frac{(H_0/L_0)_c}{H_0/L_0} && \text{if this is less than 1} \\ &= 1 && \text{otherwise,} \end{aligned} \tag{14}$$

in which $(H_0/L_0)_c$ is the critical steepness for the onset of breaking, for which Miche uses an expression derived previously by him [12]. The index "th" refers to "theoretical". The actual reflection coefficient will be smaller than r_{th} due to effects of viscosity, roughness, and permeability. Miche recommends a multiplication factor of 0.8 for smooth slopes.

Miche's assumption regarding the reflection coefficient can be expressed in terms of ξ and Iribarren and Nogales' breaking criterion. Substitution of (5) into (14) gives

$$\begin{aligned} r_{th} &= (\xi/\xi_c')^2 && \text{if this is less than 1} \\ &= 1 && \text{otherwise,} \end{aligned} \tag{15}$$

in which ξ_c' is the critical value of ξ for the onset of breaking, as distinguished from ξ_c, the value given by Iribarren and Nogales for the condition halfway between the onset of breaking and complete breaking ($\xi_c \approx 2.3$), for which the reflection coefficient is about 0.5 [7, 8]. So (15) becomes

$$\begin{aligned} r &\approx 0.1\ \xi^2 && \text{if this is less than 1} \\ &= 1 && \text{otherwise} \end{aligned} \tag{16}$$

An extensive series of measurements of the reflection coefficient of plane slopes has recently been presented by Moraes [14]. His results for slopes with $\tan \alpha = 0.10, 0.15, 0.20$ and 0.30 have been replotted in terms of r vs ξ in fig. 2. The experimental points for the four slopes more or less coincide with each other and with the curve representing eq. (16) for $\xi < 2.5$, i.e. as long as the waves break. For $\xi < 2.5$ they diverge, gentler slopes giving less reflection than steeper slopes (at the same value of ξ).

GENERAL COMMENTS REGARDING THE PARAMETER ξ

In the preceding paragraphs examples have been given of a number of characteristic surf parameters for the determination of which it is not necessary to specify both α and H/L_0, but only the combination $\tan\alpha/(H/L_0)^{\frac{1}{2}}$. It may be useful to summarize them here: a breaking criterion, the breaker type, the breaker height-to-depth ratio, the number of waves in the surf zone, the reflection coefficient (therefore also the discrimination between progressive waves and standing waves), and the relative importance of set-up and run-up. They have been collected in Table 1. Characteristic values of ξ are given in the upper row of the table. Each of the following rows indicates how one of the parameters just mentioned varies with ξ.

The recognition of the possibility that several properties can roughly be expressed as functions of ξ alone contributes to a more unified understanding of the phenomena involved. Such understanding would be deepened by further insight in the nature of the parameter ξ itself. One interpretation has already been mentioned in the preceding, when it was observed that ξ is approximately proportional to the ratio of the tangent of the slope angle to the shallow-water wave steepness. Also, ξ^{-1} had been seen to be approximately proportional to the number of wavelengths within the surf zone. This is in essence equivalent to saying that ξ is approximately proportional to the relative depth change across one wavelength in the surf zone. This interpretation is obviously relevant to the dynamics of the breaking waves, particularly with regard to their rate of deformation. It makes it plausible that ξ is of importance, but it does not prove that ξ serves as the sole determining factor for the (suitably normalized) parameters of the surf. Indeed, there are valid arguments which throw doubt on this possibility of full similarity. In this regard it is useful to consider two situations of different slope angle and wave steepness as a prototype and a distorted scale model thereof. It is well known that Froudian model-prototype similarity can be obtained even in distorted models, provided the assumption of hydrostatic pressure distribution is valid both in the prototype and in the model. Pertinent scale ratios (λ) are given in Table 2, expressed in terms of the horizontal and vertical geometrical scales and the scale of the gravitational acceleration (unity).

ξ	≈ 0.1	0.5	1.0	2.0	3.0	4.0	5.0
		breaking					no breaking
	spilling		plunging		collapsing/surging		
H_b/d_b	0.8	1.0	1.1	1.2			
$N^{*)}$	6-7 2-3	1-2	0-1	0-1			
r	10^{-3}	10^{-2}	10^{-1}	4×10^{-1}	8×10^{-1}		
		absorption					reflection
		progressive wave				standing wave	
	set-up predominant			run-up predominant			

*) number of waves in surf zone

Table 1

Variable	Symbol	Scale ratio
horizontal length	ℓ	λ_ℓ
depth	d	λ_d
gravity acceleration	g	$\lambda_g = 1$
bottom slope	tan α	$\lambda_{\tan\alpha} = \lambda_d \lambda_\ell^{-1}$
wave height	H	$\lambda_H = \lambda_d$
wave length	L	$\lambda_L = \lambda_\ell$
wave celerity	$c \sim (gd)^{\frac{1}{2}}$	$\lambda_c = \lambda_d^{\frac{1}{2}}$
wave period	$T = L/c$	$\lambda_T = \lambda_\ell \lambda_d^{-\frac{1}{2}}$

Table 2 - Scale ratios for a distorted long-wave model.

Since ξ is defined as

$$\xi = \left(\frac{gT^2}{2\pi H}\right)^{\frac{1}{2}} \tan\alpha \quad , \tag{17}$$

its scale ratio is

$$\lambda_\xi = \lambda_T \, \lambda_H^{-\frac{1}{2}} \, \lambda_{\tan\alpha} \, , \tag{18}$$

which becomes, using the values given in Tabel 2,

$$\lambda_\xi = (\lambda_\ell \lambda_d^{-\frac{1}{2}})(\lambda_d^{-\frac{1}{2}})(\lambda_d \lambda_\ell^{-1}) = 1 \quad . \tag{19}$$

In other words, a distorted long-wave model which is dynamically similar to its prototype necessarily has the same ξ as this prototype. Conversely, a distorted wave-model with the same value of ξ as its prototype is similar to this prototype if the pressure distribution in both is hydrostatic. This is not the case in breaking waves in shallow water, where some effects of the vertical accelerations must be taken into account due to the fact that the surface curvature is locally strong. Thus, the existence of similarity of the

surf in distorted models is not proved, and must be doubted to the extent that deviations from the long-wave approximations have a significant effect. Such effects are certain to be of importance for the details of the local flow patterns, but this is not necessarily the case for overall properties of the surf. The final check on this must of course be obtained empirically. In this regard it appears justified to draw the conclusion from the data presented above that the factor ξ is a good indicator of many overall properties of the surf zone, and may indeed be called a similarity parameter. The importance of this parameter for so many aspects of waves breaking on slopes appears to justify that it be given a special name. In the author's opinion it is appropriate to call it the "Iribarren number" (denoted by "Ir"), in honor of the man who introduced it and who has made many other valuable contributions to our knowledge of water waves.

REFERENCES

1. Battjes, J.A., Computation of set-up, longshore currents, run-up and overtopping due to wind-generated waves, Communications on Hydraulics, Delft University of Technology, Rep. 74-2, 1974.

2. Battjes, J.A. and Roos, A., Characteristics of flow in periodic wave run-up, in press, 1974.

3. Bowen, A.J., Inman, D.L. and Simmons, V.P., Wave "set-down" and set-up, J. Geoph. Res., 73, 8, 1968, p. 2569-2577.

4. Galvin, C.J. Jr., Breaker Type Classification on Three Laboratory Beaches, J. Geoph. Res., 73, 12, June 1968, p. 3651-3659.

5. Galvin, C.J. Jr., Wave breaking in Shallow Water, in Waves on Beaches, Ed. R.E. Meyer, Academic Press, New York, 1972, p. 413-456.

6. Goda, Y., A synthesis of breaker indices, Trans. Jap. Soc. Civ. Eng., 2, 2, 1970, p. 227-230.

7. Hunt, I.A., Design of seawalls and breakwaters, Proc. ASCE, 85, WW3, Sept. 1959, p. 123-152.

8. Iribarren, C.R. and Nogales, C., Protection des Ports, Section II, Comm. 4, XVIIth Int. Nav. Congress, Lisbon, 1949, p. 31-80.

9. Iversen, H.W., Laboratory Study of Breakers, Nat. Bur. of Standards, Circular 521, Washington, D.C., 1952, p. 9-32.

10. Kemp, P.H., The relationship between wave action and beach profile characteristics, Proc. 7th Conf. Coastal Eng., The Hague, 1960.

11. Longuet-Higgins, M.S. and Stewart, R.W., A note on wave set-up, J. Mar. Res., 21, 1963, p. 4-10.

12. Miche, R., Mouvements ondulatoires de la mer en profondeur constante ou décroissante, Ann. des Ponts et Chaussées, 114è Année, 1944.

13. Miche, R., Le pouvoir réfléchissant des ouvrages maritimes exposés à l'action de la houle, Ann. des Ponts et Chaussées, 121è Année, 1951, p. 285-319.

14. Moraes, Carlos de Campos, Experiments of Wave Reflexion on Impermeable slopes, Proc. 12th Conf. Coastal Eng., Washington, D.C., 1970, Vol. I, p. 509-521.

15. Patrick, D.A. and Wiegel, R.L., Amphibian tractors in the surf, Conf. Ships and Waves, 1, 1954, p. 397.

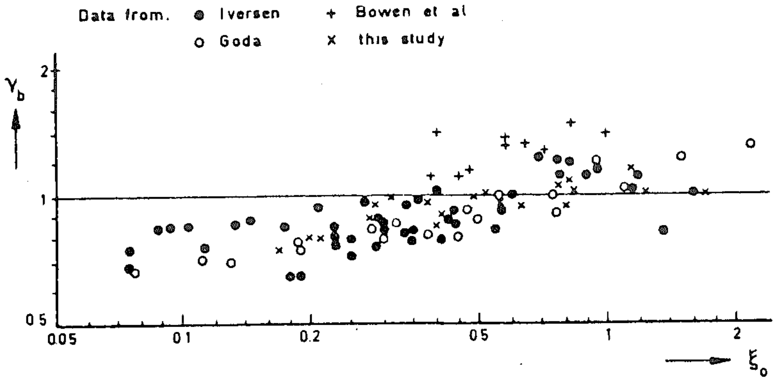

Figure 1 - Height-depth ratio at breakpoint vs. the similarity parameter.

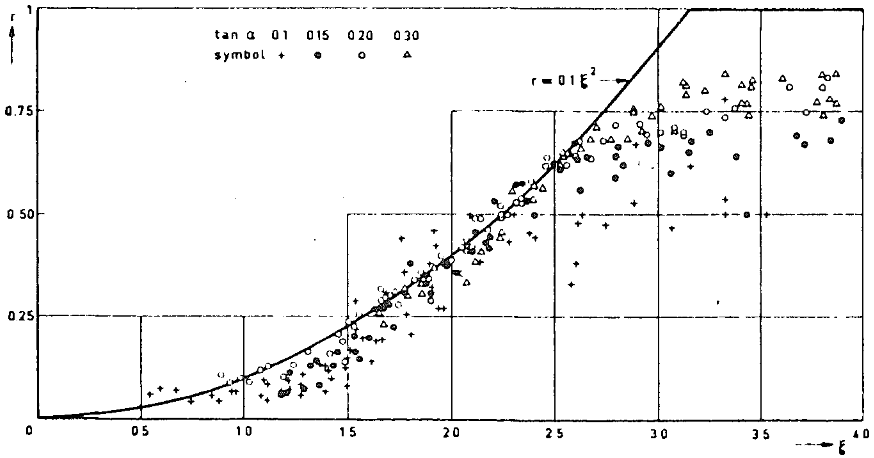

Figure 2 - Reflection coefficient vs. the similarity parameter.